

Thesis for the Master's degree in Biosciences  
Main field of Study in Marine Biology

**Stein Hegvik**

**Acoustic startle responses in European sprat  
(*Sprattus sprattus L.*) and diploid versus triploid  
Atlantic salmon fry (*Salmo salar L.*)**

60 study points

**Department of Biosciences**  
Faculty of Mathematics and Natural Sciences

**UNIVERSITY OF OSLO 10/2014**



## **Preface**

This thesis is a result of studies conducted at the University of Oslo, Marine Biological Research Station Drøbak, Norway in the period 2013-2014.

I am indebted to my supervisor Dr. Hans Erik Karlsen, director of the Drøbak Marine Biological Research Station, University of Oslo, for all his help and assistance throughout the project. Special thanks to Jens Haga, Rune Roland Hansen and Grete Sørnes at the University of Oslo and to Maria Wilson at the University of Aarhus, Denmark, for all help and all good times at the research station in Drøbak. I would like to thank prof. Ian Mayer and Dr. Thomas Frazer at the Norwegian University of Life Sciences, Veterinary High school, Oslo, and the staff at Institute of Marine Research, Matre Research Station, Bergen, for the supply of diploid and triploid salmon fry. I would also like to thank my girlfriend Christina Hansen Edwards for her support and patience. Finally, I would like to thank prof. Tom Andersen at the Section for Aquatic Biology and Toxicology at the University of Oslo for assistance with statistical analyses and Grete Sørnes and Ian Mayer for valuable comments to the manuscript.

# Contents

## Summary

<b>1. Introduction</b>	<b>7</b>
<i>Background</i>	7
<i>Hypothesis</i>	16
<b>2. Materials and Methods</b>	<b>13</b>
<i>Experimental animals and water supplies</i>	13
<i>Properties and descriptions of acoustic stimuli</i>	15
<i>Acoustic pressure sensitivity in clupeid fish</i>	16
<i>Experimental setups</i>	18
<i>Stimulus driving voltage waveforms to the vibrators</i>	22
<i>Stimulus pressure and acceleration waveforms in the swing and     the pressure system</i>	24
<i>Experimental procedure</i>	27
<i>Video analysis and statistics</i>	30
<b>3. Results</b>	<b>31</b>
<i>Startle response probabilities in sprat in the pressure and the     swing systems</i>	31
<i>Startle response latencies in sprat in the pressure and swing system</i>	33
<i>Startle response directionality in sprat in the pressure and the     swing system</i>	33
<i>Startle response probabilities in triploid and diploid salmon fry     in the swing system</i>	37
<i>Startle response latencies in triploid and diploid salmon fry     in the swing system</i>	39
<i>Startle response trajectories for diploid and triploid salmon     in the swing system</i>	39

<b>4. Discussion</b>	<b>43</b>
<i>Sensory information responsible for startle behaviours in the experimental setups</i>	43
<i>Pressure phase sensitivity of startle behaviours in sprat and the evolution of acoustic pressure sensitivity in fish hearing specialists</i>	45
<i>Startle response directionality in sprat in the pressure and swing system</i>	46
<i>Acoustic startle response latencies in sprat</i>	48
<i>Startle behaviour by diploid and triploid salmon fry in the swing system</i>	49
<i>Conslusions</i>	50
Appendix	52
References	54
<b>List of Figures</b>	
1.1 Cross section of a fish otolith organ	9
1.2 Mauthner cells of the brainstem escape network	10
2.1 Salmon erythrocytes	14
2.2 Inner ear swim bladder connection	17
2.3 Otic bulla and pre-otic membrane	17
2.4 The swing system	19
2.5 Swing system AOI	20
2.6 The pressure system	21
2.7 Voltage waveforms	23
2.8 System calibrations	25
2.9 Stimulus waveforms swing system	26
2.10 Stimulus waveforms pressure system	28
2.11 Sprat and salmon tracking	29
3.1 Sprat startle response probabilities in the pressure system	31
3.2 Sprat startle response probabilities in the swing system	32
3.3 Sprat startle response trajectories aligned	34
3.4 Sprat turning angles aligned	34

3.5 Sprat initial orientation and trajectories with acceleration	36
3.6 Sprat turning angles acceleration	37
3.7 Startle response probabilities for salmon in the swing system	38
3.8 Boxplot of salmon latency times	39
3.9 Salmon startle trajectories aligned	40
3.10 Salmon turning angles aligned	40
3.11 Salmon trajectories initial orientation and acceleration	41
3.12 Salmon turning angles acceleration	42

## **Abstract**

Fast start and short-duration acoustic startle behaviour (C-response) are performed by fish in order to successfully evade abrupt threats such as attacks by predatory fish. In the present thesis acoustic startle behaviour in the fish hearing specialist sprat and in diploid (2n) and sterile triploid (3n) fry of the fish hearing non-specialist salmon was studied in a pressure and in a swing chamber set-up. Specially designed acoustic stimulus waveforms, closely approximating a 20 Hz or a 30 Hz single cycle sinusoid of acoustic pressure and particle acceleration, were employed to reveal what acoustic parameters were eliciting and driving the escape behaviours. The set-ups mimicked key components of the acoustic signatures of charging and suction type of predatory attacks.

Acoustic startle behaviour was found to be triggered mainly by acoustic compression in sprat. The acceleration component of the sound had no effect on startle probability for sprat, but was shown to determine the directionality of startle response trajectories. Acoustic startle behaviour in diploid and triploid salmon fry was triggered by particle acceleration, and appeared to un-affected by acoustic pressure. Startle behaviours were found to be similar in triploid and diploid salmon with respect to response latency, distance and directionality. There was a marginal, but significant increased response probability for triploid salmon. Thus, triploidy did not hamper the highly complex startle behaviour.

The acoustic pulse levels in terms of pressure and particle acceleration required to elicit a startle response in sprat was approximately 30 dB (a factor of about 32) lower than for diploid and triploid salmon. It is proposed that the enhanced hearing of fish hearing specialists has evolved as adaptations for low frequency pressure sensitivity in order to detect and evade a striking predator at a greater distance than would be possible for a hearing non-specialist. Predator-prey interactions are concluded to have been a key factor in the evolution of hearing in fish.

## 1.Introduction

In nature, predator-prey interactions are continuous battles for survival among individuals, and over time they constitute an evolutionary race in which attack performance by the predator and evasive behaviour by the prey are modified and advanced within species boundaries. Precise targeting of the prey as well as stealth and speed in the attack are crucial to a predator, while for a prey it is essential to recognize the predator and its attack early enough to successfully avoid predation by performing an evasive response. In this way, predation represents a key selective force in animals for refinement of sensorimotor systems as well as a spectre of behavioural strategies to ensure survival.

There are two main types of attack behaviours recognised in fish. In the first type of attack, a striking predator by definition abruptly charges forward towards the prey, and characteristically creates frontal bow waves consisting of an initial pressure increase (compression) associated with water acceleration away from the predator (Eaton and Popper, 1995; Eaton et al., 1995). The second type of attack involves predator fish opening a large mouth and sucking in water and the prey. Contrary to a striking predator, the suction type of predation is modelled as initial water movement towards the predator associated with pressure decrease (rarefaction) (Eaton et al., 1995). With respect to acoustic signatures, the vital challenge for a prey fish is to detect and interpret an imminent attack from water accelerations and pressure changes correctly with minimum delay, and to respond quickly and adaptively by freeze behaviour and camouflage or by fast escape away from the predator in question.

Fish have two highly developed sensory systems for the detection of external water movements and pressure changes, i.e. the lateral line and the inner ear system. The lateral line system consists of numerous mechano-sensitive lateral line organs (neuromasts) scattered in the epidermis of the fish (free neuromasts) or confined inside epidermal canals (canal neuromasts) on the head of the fish, and in most species in a long canal, the lateral line, found along each side of the fish. Lateral line organs detect low frequency ( $< 100$  Hz) water movement relative to the skin of the fish. Such relative or local water flows are normally only produced when a fish is within a few cm of external objects, referred to as a sense of distant touch. Beyond these distances (cm range) the fish and surrounding water will typically either move as a unit, thereby eliminating stimulation of the lateral line system, or water

displacements along the skin of the fish will be below the activation thresholds of the lateral line organs.

In addition to the lateral line system, fish also possess a sensitive inner ear system. Each inner ear, on either side of the head, consists of three semi-circular canals, for the detection of rotational body movement, and three otolith organs named the utricle, the saccule and the lagena. Each of the three otolith organs is in essence a fluid filled sack containing a calcium carbonate otolith mechanically coupled to an epithelium of displacement and directional sensitive hair cells (Figure 1.1). A fish mostly consists of water and lives within a water environment. Therefore, a fish in a sound field will vibrate with the same amplitude, frequency and direction as the surrounding water molecules. Due to its larger density ( $\approx 3 \text{ g/cm}^3$ ) and inertia, the otolith will lag behind the acoustic vibrations of the soft parts of the fish, and thereby cause relative movement between the otolith membrane and the underlying hair cells. Consequently, the apical hair bundles of the hair cells are deflected, and the hair cells stimulated. Functionally, most otolith organs in fish behave as critically damped inertia motion detectors with resonance frequencies in the range 200-300 Hz (de Vries, 1950; Lewis, 1984; Kalmijn, 1988; 1989, Karlsen, 1992). This means that below resonance, the displacement and stimulation of the inner ear hair cells are independent of frequency and proportional to the acceleration of the fish, and thus to the incident sound particle accelerations experienced by the fish. In this way, the inner ear otolith organs in fish function as low frequency and directional sensitive acceleration detectors. They are directly stimulated by linear body accelerations, by the acceleration of gravity as well as by propagated and near field particle accelerations associated with sound and sound sources.

A second and indirect way for sound energy to reach the inner ear otolith organs involves detection of changes in acoustic pressure (see Rogers et al., 1988). This mechanism involves elastic gas-filled structures within the fish such as the swim bladder in carp fish, or the otic bullae in clupeid fish such as European sprat *Sprattus sprattus* (Linnaeus, 1758) and Atlantic herring *Clupea harengus* Linnaeus, 1758. Since gas is much more compressible than water, sound pressure variations may cause larger volume pulsations of the gas structures than the direct sound induced oscillations of the fish itself. The amplified gas bladder movements may be transmitted through the fish, and stimulate the inner ear otolith organs making the fish indirectly sensitive to acoustic pressure. Species with specialized adaptations for this type of sound pressure sensitivity, including members of the fish orders Clupeiformes, Cypriniformes and Siluriformes are referred to as fish hearing specialists. Conversely, fish



species which lack such specializations and thereby are far less or totally non-sensitive to sound pressure, are referred to as fish hearing non-specialists.

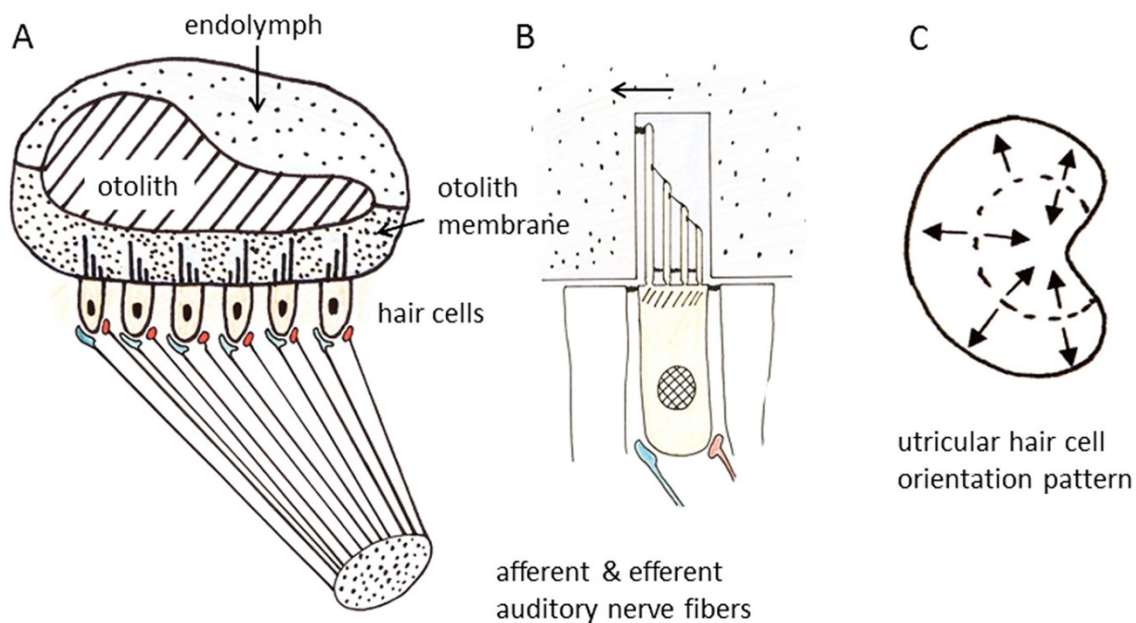


**Figure 1.1** (A) Cross section of a fish otolith organ. Each otolith organ is a vesicular structure filled with fluid endolymph and a dense otolith overlaying an epithelium of sensory hair cells. (B) Stiff, apical sensory hair bundles (stereocilia) on the hair cells protrude into small holes in the otolith membrane, and are anchored to it at the tip of the longest sensory hair in the bundle, the kinocilium. A thin water film separates the hair cells and otolith membrane. Hair cells are stimulated by hair bundle deflections in the direction of the kinocilium only, indicated by the arrow. (C) Hair cell orientation varies in the otolith epithelium making the otolith organ sensitive to overall fish displacements in different directions. (Modified from unpublished sketches by H. E. Karlsten).

It is well established that fish have an extraordinary ability to perform fast-start and short-duration escape behaviours (startle responses) in order to evade predatory attacks (see Eaton et al., 2001). Even though startle responses may be triggered by vision and lateral line stimulation, the main stimulus for eliciting this behaviour in fish appears to be acoustic stimuli activating the inner ear (see Eaton et al., 2001). Pressure is a scalar quantity in the sense that it has no direction at a single point in a medium. This suggests that pressure detection alone is an insufficient cue for performing adaptive escape behaviours away from threats. Directional information from the lateral line, the inner ear or the visual system may be needed as well.

In nature, startle responses are initiated when either of two huge spinal neurons, called Mauthner cells, are activated (see Faber et al., 1989; 1991; Korn and Faber, 1996; Zottoli and Faber, 2000; Eaton et al., 2001). Mauthner- or M-cells are integrating brainstem neurons,

which receive a wide spectre of direct sensory information (Figure 1.2). They connect directly to spinal motor neurons innervating most contra- and ipsi lateral body muscles. When one of the M-cells reaches its threshold, the action potential created triggers a contraction of contra lateral trunk musculature and at the same time an inhibition of

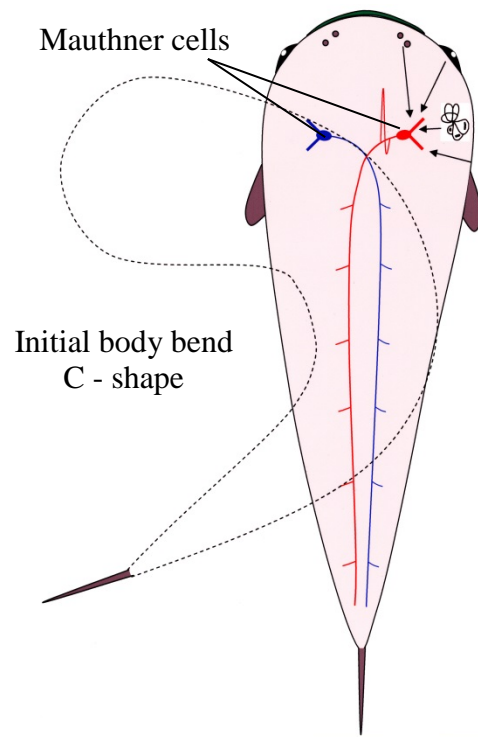


**Figure 1.2** Sketch illustrating the two Mauthner cells of the brainstem escape network (BEN). Mauthner cells and their brain stem homologs, integrate neural input from sensory organs. When activated they stimulate contra lateral body musculature and drive startle behaviour. How M-cells and the rest of the super-fast BEN determine the correct initial C-bend away from threatening stimuli is still largely unknown. (Modified from unpublished sketch by H. E. Karlsen).

ipsi lateral body musculature. The consequence of these twin responses is an initial C-bend of the fish body to the left or right. The M-cells are key components of a large neural brainstem escape network named the BEN.

As a super-fast decision making (left or right) neural network, the BEN has been extensively studied by electrophysiological techniques for the last 40 years, and much is thus known about the neuronal mechanisms involved in the startle response (see Zottoli and Faber, 2000). On the other hand, much is still unclear about what acoustic cues in particular are driving startle responses in fish, and whether startle behaviour differs significantly in fish depending on their auditory capabilities, background noise levels and more. In one behaviour

study (Karlsen et al., 2004) a specially designed experimental setup called a swing system was employed to study acoustic startle responses in the fish hearing specialist roach *Rutilus rutilus* (Linnaeus, 1758). Surprisingly, and in contradiction to predictions of widely accepted neurological BEN models in fish, it was found that acoustic startle behaviours were triggered by compression only and very rarely by rarefaction. In addition to pressure phase, the roach were detecting and responding to sound particle accelerations since this guided startle response directionality in the swing system. Understanding how acoustic pressure and particle acceleration drive escape behaviour in fish hearing specialists may reveal how and why an acute sound pressure sensitivity evolved in large groups of fish.

In the present master thesis acoustic startle behaviour was further examined in the marine species the sprat, and the Atlantic salmon *Salmo salar* (Linnaeus, 1758). Sprat is a fish hearing specialist and sensitive to both sound particle acceleration and sound pressure, while the Atlantic salmon is a fish hearing non-specialist and sensitive to sound particle acceleration only. In addition to a new version of the experimental swing chamber, a newly designed pressure chamber and a new stimulus waveform was employed allowing, for the first time, for controlled acoustic stimulations by pure rarefaction and by pure compression pulses alone. The salmon studied in the thesis work were both normal diploid (2n) and sterile triploid (3n) fry, obtained from the same sibling population of farmed Atlantic salmon (see *Experimental Animals and water supplies*). There is increasing interest in the use of sterile triploid salmon in aquaculture for two main reasons. Firstly, the use of triploids would address the environmental concerns associated with escaped farmed fish interbreeding with wild salmon stocks, and secondly would mitigate the problems associated with early precocious sexual maturation. Compared to diploid salmon, the size of cells and cell nuclei in triploid salmon is increased by close to 50%. Information on how this difference in cell size can affect brain and sensory functions is currently lacking. Startle responses are complex behaviours involving highly specialized sensory organs and neural networks, and appear well suited as reference behaviour for revealing possible general brain malfunctions in triploid salmon. One of the goals of this master thesis was thus to evaluate whether ploidy state (2n or 3n) influenced the acoustic startle response in salmon fry, and if so to compare diploid and triploid salmon with respect to critical qualitative aspects of their acoustic escape behaviour such as threshold levels, response latencies and escape distances.

As such, the primary aims of the thesis and the hypotheses which was sought to be answered were the following:

**H01:** Acoustic startle behaviour is elicited with equal probability by sound pressure and by sound particle acceleration in sprat and diploid and triploid salmon fry.

**H02:** Acoustic startle behaviour is elicited with equal probability in sprat by acoustic compression, mimicking a charging predator attack, and by acoustic rarefaction, mimicking a suction predator attack.

**H03:** Acoustic startle behaviours in diploid and triploid salmon do not differ with respect to their startle threshold level, startle latency, startle distance and startle directionality.

## 2. Materials and Methods

### *Experimental animals and water supplies*

In late June sprat, 4-5 cm long, were present in large number close to the surface in the local harbour of the University of Oslo, Marine Research Station Drøbak, where all experiments were performed. Sprat were caught using fine masked nets to drive small shoals together such that the sprat could be collected in 30 l plastic buckets without being touched or injured in any way. Immediately after capture, they were transported inside the station, and gently transferred to 500 l storage tanks with continuous flow of salt water from a depth of approximately 3 m. The water temperature used for fish storage and in the experiments was the same as the temperature (15 °C – 22 °C) in the water from where the fish originated. Diploid and triploid salmon were produced at the Matre Field Station run by the Institute of Marine Research (IMR) in Bergen. The young salmon fry (1-5 days old) were transported in temperature controlled containers by car from Matre (Bergen) to the Marine station in Drøbak, and stored separately in 100 l glass aquaria. The fresh water used was ordinary tap water which was charcoal filtered and supplied with sodium chloride corresponding to a concentration of 0,5 mM and calcium chloride corresponding to a concentration of 0,2 mM. Fresh water was prepared in batches of 700 l in a 1,5 m x 1,5 m x 0,6 m experimental water storage tank. It was aerated and temperature regulated to 12-14 °C before being supplied to the fish in storage tanks or experimental test chamber. As development of the salmon larvae advanced, they were fed dry pellet food as well as fresh water zooplankton caught in fresh water lakes in the vicinity of the Marine station in Drøbak.

In order to secure that the salmon fry examined were true triploid, a random selection of 10 diploid and 10 triploid fish examined in the behaviour tests were euthanized, blood smears established for each individual, and erythrocytes nucleus sizes recorded (Figure 2.1). The surface area of 15-20 cell nuclei were measured in every individual fish using the image analysis software ImageJ 1.49d (National Institutes of Health, USA). The overall mean size of diploid erythrocyte nucleus was 28,4  $\mu\text{m}^2$  while it was 41,3  $\mu\text{m}^2$  for the triploid, making up a 45% mean nuclei size increase in triploids. The difference between

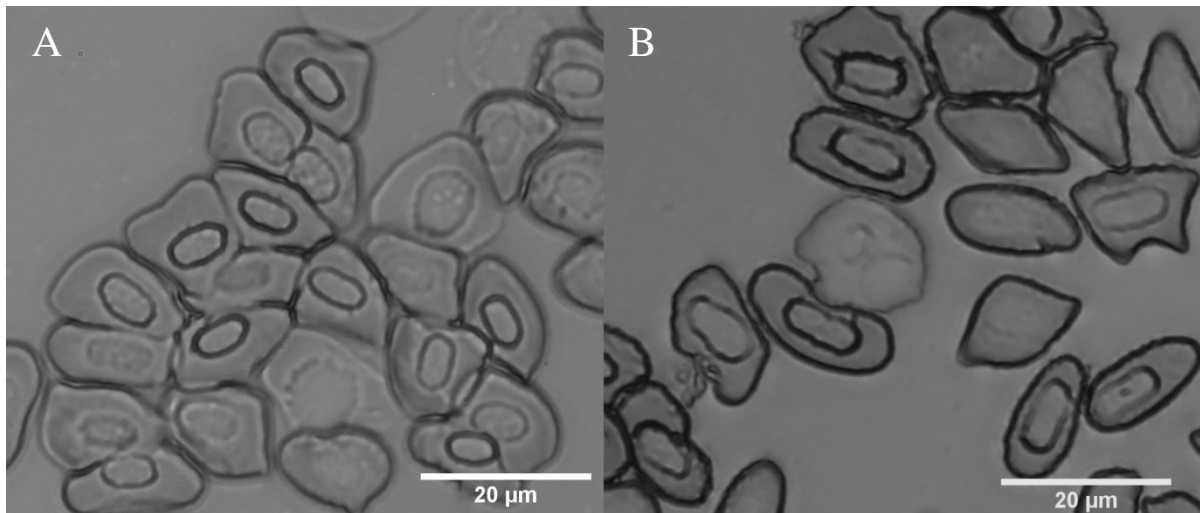


**Figure 2.1.** Microscopy image of erythrocytes in diploid (A) and triploid (B) salmon fry. Triploidy results in approximately 50 % larger cells and cell nuclei. This was true for the triploid salmon group examined in the thesis work, confirming a successful triploidy production process.

diploids and triploids were highly significant in all instances (pairwise two-tailed t-tests,  $p < 0,001$ ). The observed cell parameter differences coincide with previous findings for erythrocytes in triploid and diploid fry (Benfey & Sutterlin, 1984).

Acoustic startle responses were examined with the experimental fish inside one of two small test chambers, further described in the next sections. During acclimatization periods with no testing, the test chamber was slowly circulated at approximately 50 ml/min with water from the water storage tank containing salt water or prepared fresh water. In detail, a small aquaria pump submerged in the storage tank fed water to a second 30 l supply tank also placed inside the storage tank. The 30 l supply tank fed water through a hose to the test chamber, and had a constant overflow level which was adjusted to be about 40 cm above the inlet of the test chamber. This secured a constant gravity driven flow of water through the test chamber. The height of the outlet from the test chamber was adjusted to give a pressure inside the test chamber of 20-30 cm of water, comparable to the pressures in the test fish storage aquaria. A total of approximately 120 fish were studied in the experiments, which were conducted in accordance with the Norwegian Animal Act of 1974 and the Regulation on Animal Experimentation of 1996.

## *Properties and descriptions of acoustic stimuli*

All objects or media in nature have the physical property of elasticity. This means that any object moving or vibrating in a medium such as water will cause alternating elastic movements of the media molecules, referred to as sound particle motions. Linked to the particle oscillations there will be alternating compressions and rarefactions of the media, i.e. sound pressure variations. Thus, sound has a dualistic nature, and consists of both particle motions and pressure changes. Particle motions are vector quantities, and are measured as direction and as displacement (m), velocity ( $\text{ms}^{-1}$ ) or acceleration ( $\text{ms}^{-2}$ ). Sound pressure is a scalar quantity and measured in Pascals ( $\text{Pa} = \text{Nm}^{-1}$ ). In studies of fish hearing, sound pressures levels are by convention presented in decibel values relative to a reference pressure of  $10^{-6}$  Pa ( $1\mu\text{Pa}$ ) according to the equation:

$$\text{Number of dB (re } 1 \mu\text{Pa)} = 20 \log \frac{\text{measured pressure (Pa)}}{1 \mu\text{Pa}}$$

At large distances from a sound source and any reflecting surfaces there is a simple linear relation between the levels of sound pressure and sound particle motion. This situation is referred to as far field sound. Close to a sound source however, such as a fish charging forward in an attack, particle motions will be greatly increased relative to pressure levels, and consist of particle motions linked to propagating pressure changes as well as particle motions due to net displacements of the medium. The non-elastic or hydrodynamic water movements close to a sound source are called near field effects. In general, significant near field water movements extend to distances of approximately  $\lambda/2\pi$  from the sound source. This compares to approximately 12 m at a frequency of 20 Hz. Since all fish are directly sensitive to particle acceleration, knowledge about near field effects may be of vital importance in the understanding of how and why fish respond to different types of sound. Since predator-prey interactions occur in the near field, they will encompass a larger ratio of particle acceleration to pressure than for far field sound. Such near field conditions were mimicked in the experimental test chambers employed in the thesis.

An attack by a predatory fish creates a sound pulse as opposed to more continuous sound from for instance a passing vessel. Evasive startle responses by prey fish to impulse sound typically occur with short latency (10-50 ms) in the time domain and not over several cycles in the frequency domain. As shown below, the stimulus sound pulses employed in the

current master thesis closely approximated single cycle sinusoids of 20 Hz and 30 Hz particle acceleration and pressure. The pulses were created and chosen in order to mimic the key low frequency water displacement components known to be created during predatory fish attacks (Bleckmann et al., 1991), and in order to be able to examine whether behaviour responses were driven differently by the initial pressure phase, i.e. by charging or suction type of predators. Impulsive sound may be characterized but calculating the total pulse energy, by zero to peak (0-p) pressure amplitude and more. Continuous sound is typically measured as pressure amplitude rms (root mean square). The amplitude rms equals amplitude (0-p)/ $\sqrt{2}$ , and is commonly used since integrating the amplitude rms value over time gives sound energy directly. In the present master thesis pressure and particle levels are presented as amplitude rms. It should be noted that while sound pressure in fish studies by convention are denoted in decibels relative to 1  $\mu\text{Pa}$ , the reference pressure in the study of human hearing is 20  $\mu\text{Pa}$ . In addition, the acoustic impedance of water is very different from that of air. Taken together, this means that a sound of 120 dB re 1  $\mu\text{Pa}$  in water has the same energy as the same sound at approximately 60 dB re 20  $\mu\text{Pa}$  in air. It is thus necessary to subtract approximately 60 dB in order to compare the decibel values of the two sounds with respect to energy ( $\text{J}/\text{m}^2$ ) and intensity ( $\text{W}/\text{m}^2$ ).

#### *Acoustic pressure sensitivity in clupeid fish*

Clupeid fish like sprat possess a pair of gas filled vesicles called otic bullae (Figure 2.2) in close proximity to the utricles in the two the inner ears (Allen and Blaxter, 1976; Blaxter and Denton, 1976; Popper and Platt, 1979). Each bulla is divided into gas-filled and liquid-filled parts by an elastic membrane called the pre-otic membrane (Blaxter et al., 1981). The gas filled part of each bulla is connected to the swim bladder by a pre-coelomic duct allowing the swim bladder to act as a gas reservoir for the bullae, and thereby to ensure an equal pressure in the bullae and the surrounding water (Allen and Blaxter, 1976).



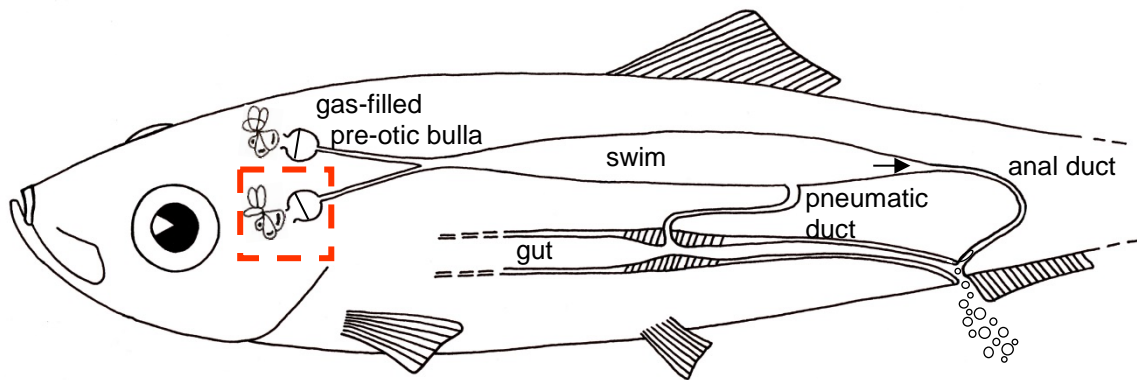


**Figure 2.2.** The special adaptation for pressure sensitivity in Clupeids include forward swim bladder extensions in the form of two gas-filled bullae which are closely associated with the utricle otolith organs of the two inner ears (shown in the red square). The close connections means that sound induced vibrations of pre-otic membranes within the bullae effectively stimulate the utricle organs (see Figure 2.3 for more details). (Sketch by H. E. Karlsen).

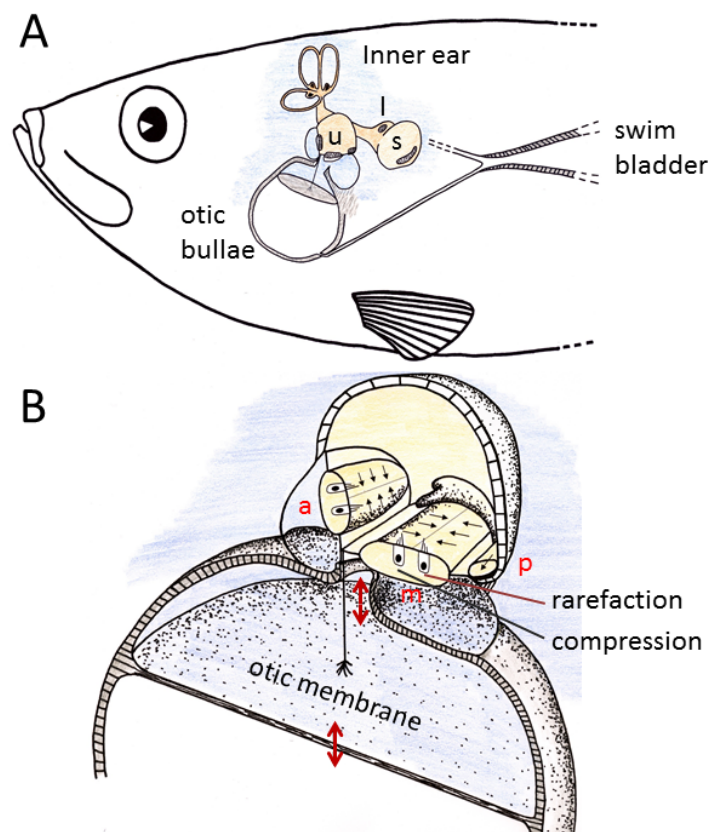


**Figure 2.3.** The figure shows part of the otic bulla-ear connection in clupeid fish (A). The gas and fluid filled parts of the otic bullae are separated by an elastic pre-otic membrane. The pre-otic membrane oscillates in response to external pressure changes, causing alternating water movement through the fenestra of the bullae and thereby stimulation of utricular hair cells. Some acoustic nerve fibres have been shown to respond specifically to either compression or to rarefaction (B). (Modified from unpublished sketch by H. E. Karlsen).

The upper part of the bullae (see Figure 2.3B) contains perilymph, and is connected to the labyrinth via a fenestra in the upper wall of the bulla (Blaxter et al., 1981a). Pressure changes acting on the fish cause displacements of the elastic bullae membrane which lead to liquid displacements of the perilymph, and stimulation of sensory hair cells in the utricle (Blaxter et al., 1981b). Importantly, the utricle contains two groups of oppositely oriented hair cells which are stimulated by sound compression and rarefaction respectively (Denton and Gray, 1980; Denton and Gray, 1993). Clupeids may thus have the ability to respond specifically and differentially to pressure phase, such as for charging and suction predators.

### *Experimental setups*

Test fish were studied in two separate experimental setups, each designed to create controlled sound pulses mimicking key components in the acoustic signatures of a charging and a suction type of predator, respectively. The two setups will be referred to as the *swing system* and the *pressure system* in this thesis. The experimental swing system (Figure 2.4) was developed to study the combined effects of low frequency linear accelerations and pressure on fish behaviour. Earlier versions of the setup was employed to document the existence of infrasound hearing in fish (Karlsen, 1992a; b), and to show the presence of infrasound induced startle behaviour in the Otophysan hearing specialist roach (Karlsen et al., 2004). A new and slightly enlarged version of the swing system was employed in the present thesis, illustrated in Figure 2.4A. It consisted of a thick-walled (20 mm) Perspex test chamber with inside dimensions 50 cm×25 cm×13 cm, corresponding to a volume of 16,3 l. The top lid of the test chamber was transparent, and it could be tightly sealed by locking screws. Video recordings of fish behaviour were performed at 50 frames/s (Handycam HDR-PJ740, Sony, Japan), and for some experiments at 1000 frames/s (MotionBlitz EoSens Mini1, Mikrotron, Germany). A water inlet was present in one of the end walls of the chamber, and a water outlet at the other end. This made it possible to adjust for a small flow through the test chamber, and to keep this free from any air bubbles. The test chamber was suspended by four 27 cm long steel wires from a solid steel framework attached to a steel base firmly attached to a 150 kg concrete block. In order to minimize background vibrations of the test chamber, the concrete block was placed on a 20 cm layer of dry sand

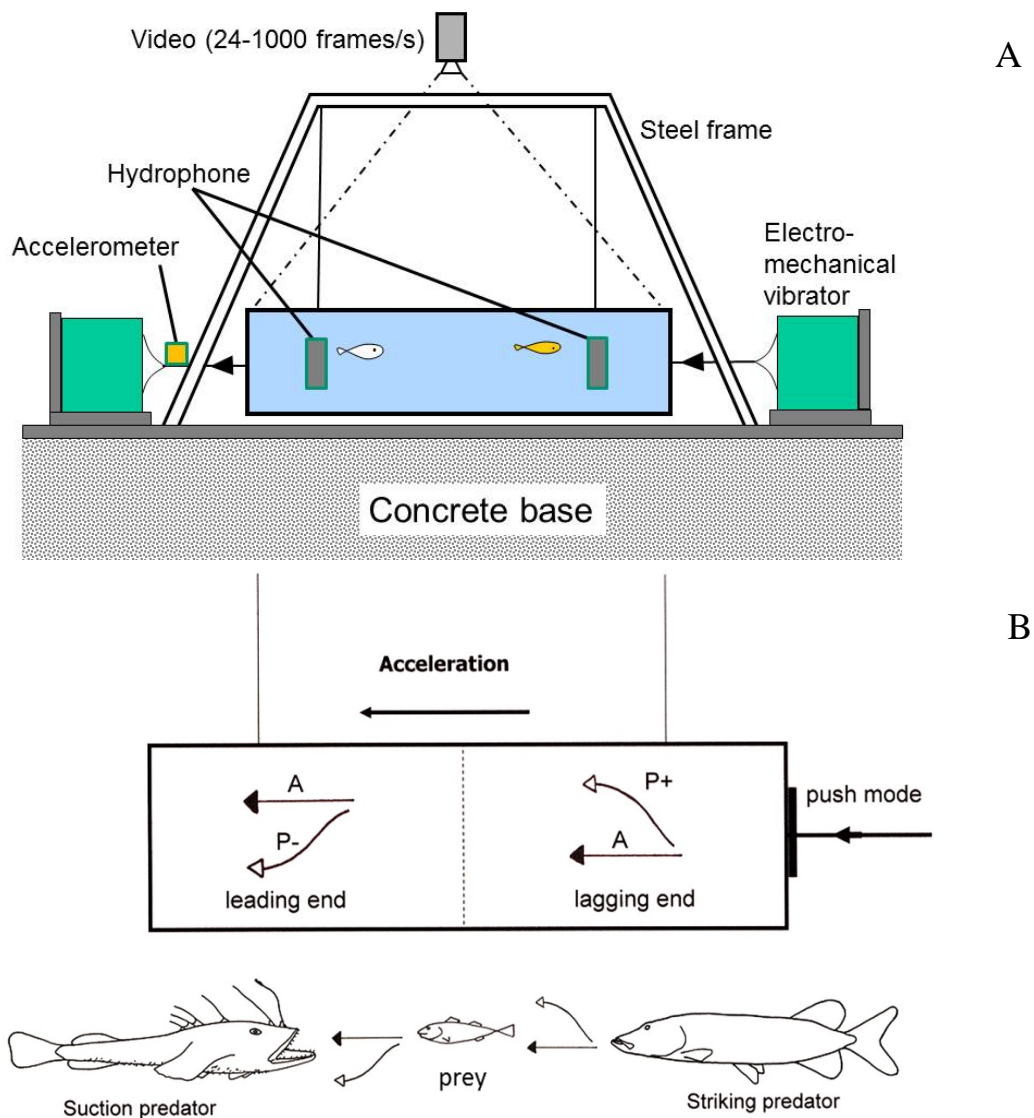


**Figure 2.4.** (A) The experimental swing system consisted of a water filled Perspex chamber suspended by four steel strings from a solid steel frame and driven by two electromagnetic vibrators. The steel frame was welded to a steel base plate, which was firmly attached to a large mass concrete block resting on dry sand. The horizontal movements of the swing chamber were measured with an accelerometer, and pressures created inside the chamber were measured with hydrophones. The behaviour of the experimental fish inside the test chamber was monitored by video. (B) Acceleration of the swing chamber caused combinations of acoustic particle accelerations and pressures mimicking the acoustic signatures of charging and suction type of predatory fish attacks. (Modified from sketches by H. E. Karlsen).

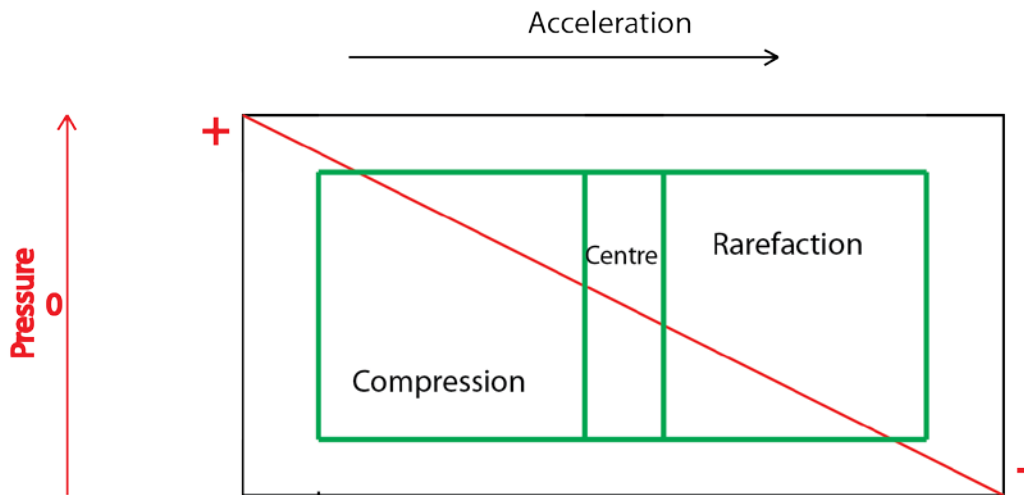


**Figure 2.5.** Three areas of interest (AOIs) were chosen for recording of acoustic startle behaviours in the swing chamber, as illustrated from above by green lines in the figure. The red line represents the pressure gradient across the chamber, i.e. initial compression in the lagging half, initial rarefaction in the leading half and a centre zone with limited pressure changes. The chamber outline is represented by the black lined square.

poured directly onto a concrete basement floor which was in direct contact with solid ground bedrock. The background accelerations of the experimental apparatus have previously been measured in 1/3 octave bands using a Brüel and Kjaer vibrations meter type 2511 (see Karlsen and Sand, 2001). In the frequency range 0,3 Hz – 1 kHz they were found to be below  $10^{-6}$   $m/s^2$  or more than 30 dB below known infrasonic auditory acceleration thresholds of approximately  $5 \cdot 10^{-5}$   $m/s^2$  in fish (see Sand and Karlsen, 2000) . The background pressure variations in the swing chamber were below 60 dB re 1  $\mu Pa$ , measured in the centre of the chamber in 1/3 octave bands in the frequency range 10-200 Hz. Background noise levels were thus well below the stimulus levels employed in the thesis, and did thus not mask behaviour responses or behaviour thresholds values. The test chamber was accelerated by two electromagnetic vibrators (Derrition VP3, Riverside, CA, USA). The vibrator each had a mass of 23 kg, and were bolted to the steel and concrete block and connected to the end wall of the suspended swing chamber by a horizontally aligned metal shaft. During experiments, initial accelerations of the swing chamber were to the left or to the right, and caused particle accelerations associated with an initial pressure decrease in the leading half and particle acceleration associated with initial pressure increase in the lagging half. In this way the swing chamber mimicked water movements created by suction and charging predatory fish attacks (Figure 2.4B).

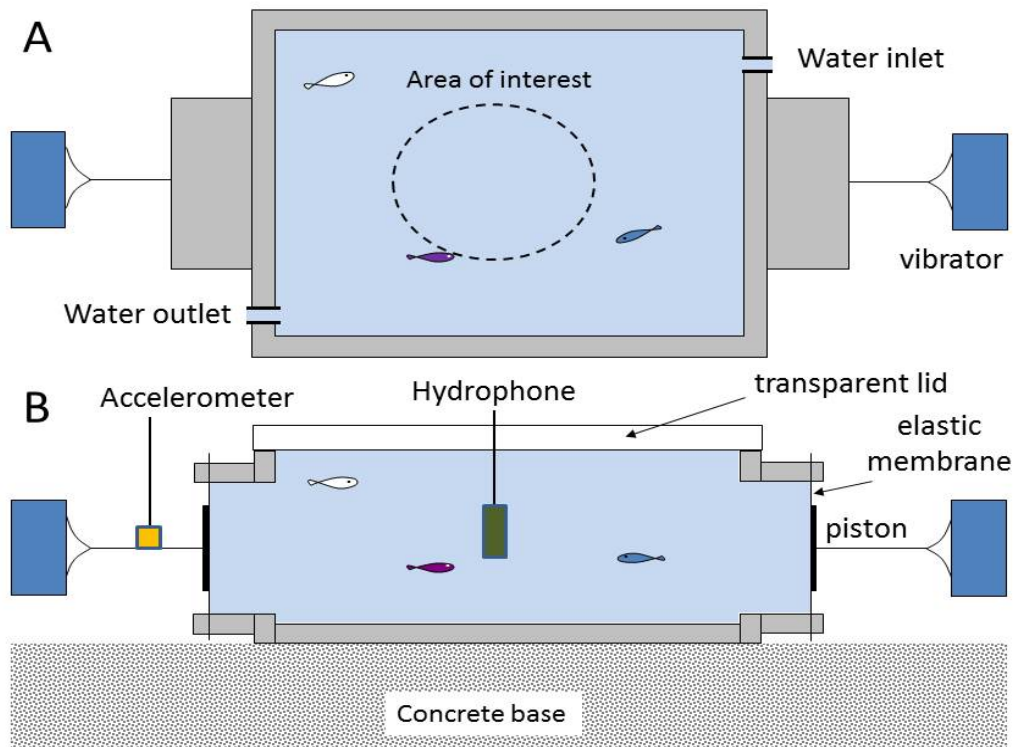


**Figure 2.6.** The pressure chamber system employed in the experiments was a thick walled (20 mm) aluminium chamber with a similar thick walled aluminium cylinder attached to and covering openings in each of the end walls. The end opening of each cylinder was fitted with a sealing rubber membrane attached to an aluminium piston and an electric vibrator. The top of the test chamber had a 5 cm thick Plexiglas transparent lid which made it possible to check for air bubbles and to video record the behaviour of the experimental fish. The vibrators were operated in pressure mode, i.e. both vibrators pushing to create uniform compression inside the chamber or both vibrators pulling to create rarefaction. In displacement mode operation, the driving voltage waveform to one of the vibrators was inverted making them operate in a push and pull mode. (Modified from sketches by H. E. Karlson).

A diagram of the experimental pressure system is shown in Figure 2.6 It consisted of a thick-walled (20 mm) aluminium chamber with the inside dimensions 70 cm x 50 cm x 18 cm corresponding to a volume of 63 l. In the centre at each end wall there was a 13 cm in diameter circular hole fitted with a similar inner diameter thick-walled (20 mm) aluminium cylinder. Each cylinder was firmly sealed by a rubber membrane. Aluminium pistons with 12 cm in diameter end plates were vulcanized to the elastic membranes, and connected by thin (4 mm in diameter) metal shafts to electric vibrators (Derritron VP 2MM, Riverside, CA, USA). The top of the aluminium chamber was a 4 cm thick and transparent Plexiglas plate, which was firmly attached to the aluminium chamber walls by 26 peripheral and evenly spaced locking screws. As for the swing chamber, video recordings of fish behaviour were performed

at 50 frames/s (Handycam HDR-CX740VE, Sony, Japan), and for some experiments at 1000 frames/s (MotionBlitz EoSens mini1, Mikrotron, Germany). During experiments, the aluminium chamber and cylinders were completely filled with water. A water inlet and outlet allowed for slow circulation of the chamber and for escape of all air.

The pressure chamber could be operated in pressure mode or displacement mode. In pressure mode, the same voltage waveform was delivered to both vibrators, i.e. both pushing or both pulling. This mode of operation created pressure changes associated with relatively small particle accelerations inside the chamber. In displacement mode, the voltage waveform to one of the vibrators was inverted. In this push and pull mode, pressure changes within the test chamber were associated with much larger particle accelerations. The wavelengths for the 20-30 Hz sound pulses employed in the thesis were above 75 m, and thus far longer than the effective length (70 cm) of the pressure chamber. As a result, uniform pressure changes were expected to be created inside the pressure chamber. By switching between pressure mode and displacement mode, it was possible to determine whether behaviour responses close to threshold were elicited and driven by pressure or by particle acceleration.

In order to minimize disturbances, the experimental swing chamber and the pressure chamber were placed inside separate sound isolated test rooms, while the investigator was in an adjacent control room conducting the experiments. All the stimulation and data recording instruments were in the control room, except for the electrical vibrator, the video camera and the acceleration and pressure transducers which were all in the test rooms. Water supply tanks to the setups were placed in additional separate and temperature regulated rooms adjacent to the test rooms.

#### *Stimulus driving voltage waveforms to the vibrators*

The driving voltage waveforms to the vibrators were designed in the software Sigmaplot version 11 (Systat Software, Inc, USA) and the software Spike 2 version 7.1 (Cambridge Electronic Design LTD, UK), and delivered by analogue to digital converters type Micro 1401 (Cambridge Electronic design LTD, UK). The waveforms were level regulated in decibel steps by an attenuator, and subsequently amplified by a specially built (Trond Reppen, University of Oslo) 40 Watt DC (direct current) power amplifier. The power amplifier was set at full gain during the experiments in order to eliminate any electric switch on-off of transients.

Two set of stimulus voltage waveforms were used in the experiments (Figure 2.7). In order to achieve a smooth onset without any initial acceleration or pressure stimulus transients, the driving voltage waveform for the swing chamber setup was a 20 Hz single cycle sine wave which was DC shifted one peak value and phase shifted  $-90^\circ$  (Karlsen et al., 2004) (Figure 2.7B). The waveform followed the general equation:  $(\omega - \omega \cos \omega t)$ , where  $\omega$  equals the angular velocity ( $2\pi f$ ).

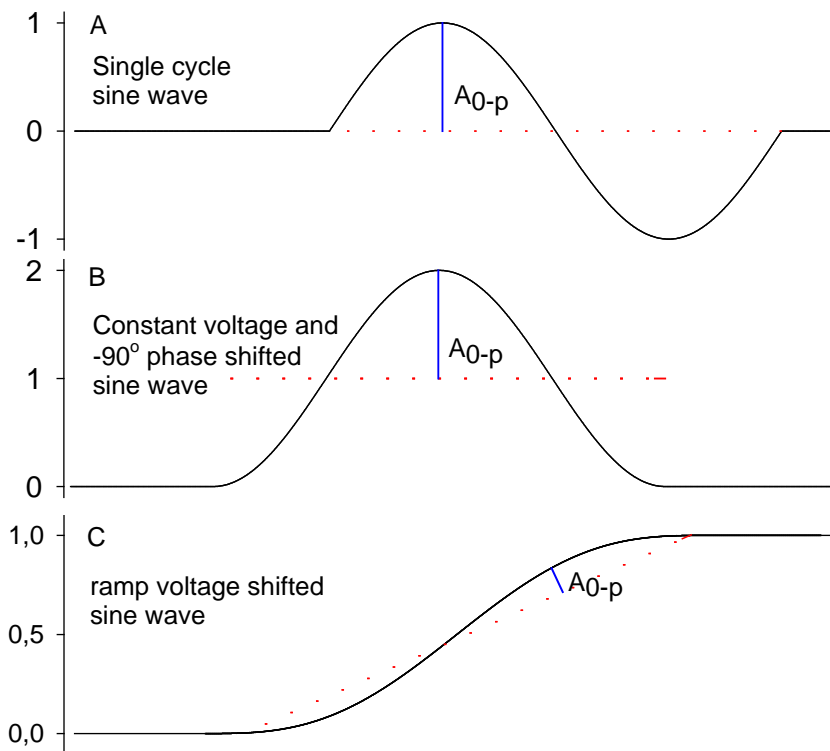


**Figure 2.7.** (A) A normal single cycle sine wave with 0-peak amplitude indicated by the blue bar. The dashed red bar shows the single cycle duration. (B) For the swing system the driving voltage waveform was a single cycle sine wave which was DC shifted one peak amplitude value and phase shifted  $-90^\circ$ . (C) For the pressure chamber system the driving voltage waveform designed was an initial negative or a positive ramp shifted single sine wave.

For the pressure system, displacements of the connecting pistons and the elastic membranes were found to largely follow the driving voltage waveform to the electromagnetic vibrators at 20 Hz. Since a main objective of the current study was to examine effects of pressure phase on startle behaviour, the ideal stimulus pressure waveform would be a harmonic cycle of pure compression or pure rarefaction with respect to the resting pressure. Such a waveform must follow the equation  $(\omega - \omega \cos \omega t)$ . Since the derivative of displacement equals velocity and

pressure, a new driving voltage waveform for the pressure chamber system was created to be the integral of the pure compression or rarefaction waveform, i.e. a waveform following the equation:  $\omega t - \sin\omega t$  (Figure 2.7C). For one harmonic cycle this waveform represented a DC voltage shift from zero to  $2\pi$  (Figure 2.7C). During actual stimulations it was thus connected to a DC voltage of  $2\pi$  lasting for 10 s followed by a return stimulus waveform to zero following the equation  $-(\omega t - \sin\omega t)$  (see Figure 2.10).

#### *Stimulus pressure and acceleration waveforms in the swing and the pressure system*

Startle behaviours of the test fish were recorded in limited areas of interest (AOI) in the leading half, the lagging half and in the centre of the swing chamber, respectively. Pressure waveforms and levels were thus measured by hydrophones placed in the centre of the areas of interest, while overall accelerations of the swing chamber were measured by accelerometers (Entran EGCS-A2-2, Les Clayes-sous-Bois, France) attached to the metal axis connecting the vibrators to the test chamber. Corresponding acceleration and pressure values measured for the 20 Hz and 30 Hz DC and phase shifted driving voltage waveforms are shown in Figure 2.8. An initial acceleration of the swing chamber of  $8 \cdot 10^{-2} \text{ ms}^{-2}$  at 20 Hz corresponded to an initial pressure level of approximately 140 dB re 1  $\mu\text{Pa}$  in the AOI within the leading and lagging half of the chamber. The particle accelerations of a propagating sound wave of frequency 20 Hz and a pressure level of 140 dB re 1  $\mu\text{Pa}$  is approximately  $8 \cdot 10^{-4} \text{ ms}^{-2}$ . Thus, it was clear that the overall acceleration of the swing chamber far exceeded the elastic particle accelerations within the chamber due to pressure changes. Therefore, the particle accelerations experienced by the fish during testing were considered to be equal to the overall acceleration of the test chamber (measured by the accelerometers), and thus essentially the same in the areas of interest in the leading, lagging and centre portion of the swing chamber, respectively. In the centre of the swing chamber, the initial pressure changes (first 100 ms) were very low and within background pressure levels in the test chamber of approximately 60 dB re 1  $\mu\text{Pa}$ . Since the acceleration of the swing chamber for a given pressure level, exceeded those of a far field sound (Figure 2.8), the acceleration of the fish during testing contained a clear near field component, i.e. comparable to a what would be experienced during predatory attacks in the wild.



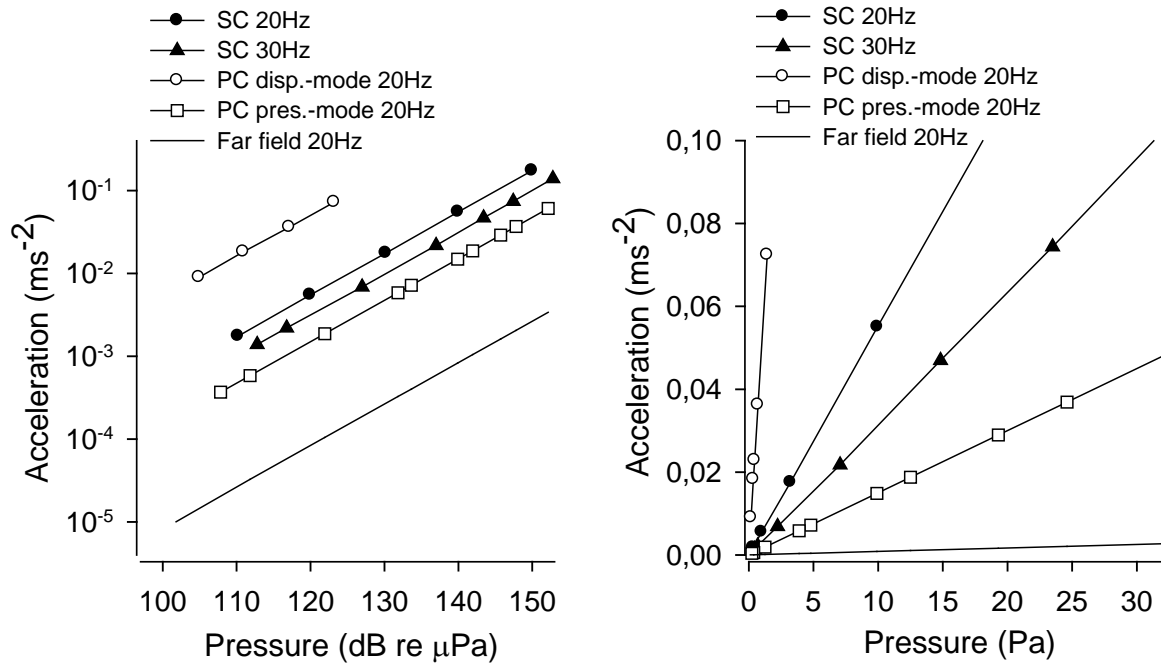


**Figure 2.8.** Corresponding pressure and acceleration values measured in the AOIs in the swing chamber and the pressure chamber. (A) Data presented in log-log scale for increased clarity. (B) Data presented in a linear scale to show convergence of all calibration curves to the origin. In (A) it is clear that particle accelerations of the swing chamber as well as the pressure chamber pistons far exceeded particle accelerations of a propagating far field sound wave. Stimulations thus contained a near field component comparable to what a fish would experience during predatory attacks in nature. For the pressure chamber the ratio of particle accelerations and pressure varied greatly between pressure and displacement mode of operation.

Corresponding stimulus acceleration and pressure waveforms for the swing chamber are shown in Figure 2.9. The stimulus pressure waveform measured inside the AIO of the lagging half of the swing chamber is shown in Figure 2.9B. It closely approximated a 20 Hz single frequency sinusoid. As expected, the pressure waveform for the AIO in the leading half was similar in shape and opposite in phase to that of the lagging half. Startle responses occurred within 20-60 ms, and could thus readily be assigned to pressure phase. The stimulus pressure waveforms recorded by the highly sensitive Sensor hydrophone (Figure 2.9D) were slightly distorted due to low pass filtering and pre-amplification of the signal within the hydrophone head stage. Still, peak pressure levels measured by the two

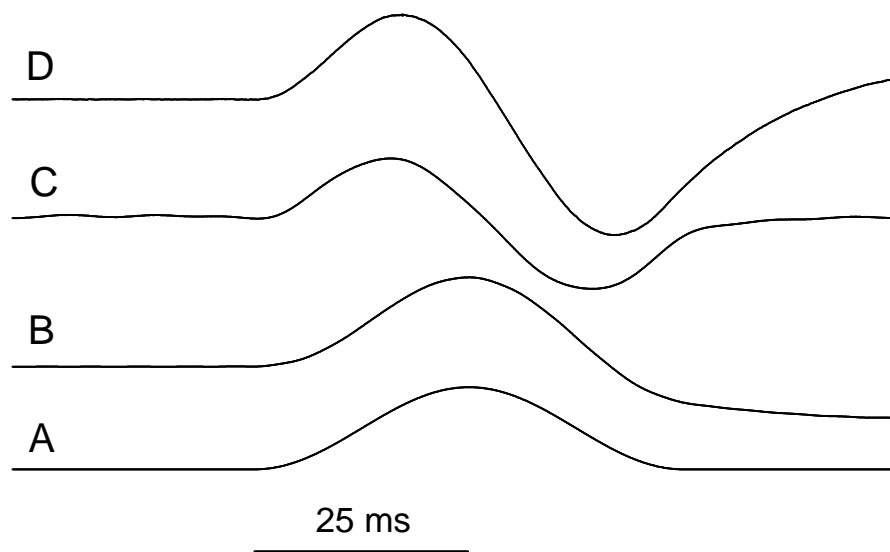


**Figure 2.9.** Stimulus waveforms recorded for the swing system at 20 Hz stimulation. All waveforms were unfiltered to avoid phase distortions. (A) For all experiments performed, the driving voltage waveform to the vibrator was a single cycle sinusoidal voltage which was D.C. shifted one peak value and phase shifted to start at  $-90^\circ$ . (B) Pressure waveform measured in the AOI in the lagging half of the swing chamber with the Reson hydrophone, i.e. without distortions from pre-amplification and filtering. The waveform closely approximated a 20 Hz single cycle sinusoid. The pressure waveform measured in the leading half of the swing chamber was identical in level but inverted  $180^\circ$ . (C) As for the recorded pressure changes, the initial acceleration of the swing chamber closely approximated a 20 Hz single frequency sinusoidal waveform. This constituted the overall acceleration stimulus the experimental fish experienced, see main text for further details. (D) Pressure waveforms recorded by the highly sensitive Sensor hydrophone. The waveform was slightly distorted due to low pass filtering and pre-amplification of the signal within the hydrophone head stage

hydrophones employed were within 4 dB of each other for all intensities examined. The acceleration waveform for the test chamber is shown in Figure 2.9C. It also closely approximated a 20 Hz single frequency sinusoid. In addition to phase, startle responses recorded were all assigned to the direction of the initial acceleration, which shifted after approximately 25 ms (Figure 2.9C).

Corresponding particle acceleration and pressure waveforms for the AOI in the centre of the pressure chamber is shown in Figure 2.10. The specially designed 20 Hz stimulus

driving voltage waveform to the vibrators is shown in Figure 2.10A. Particle accelerations within the pressure chamber, as measured by the accelerometers attached the connecting pistons of the set-up, are shown in Figure 2.10B. The stimulus acceleration waveform closely approximated a 20 Hz single cycle sinusoid. The corresponding pressure waveform, measured without distortions from pre-amplifications or filtering by the Reson hydrophone, is shown in Figure 2.10C. The waveform closely approximated a pure 20 Hz single cycle sinusoidal compression waveform followed after 10 s by a similar type of rarefaction waveform. Thus the stimulus pressure waveform allowed for controlled examinations of whether startle behaviours were elicited by compression (charging predation) or rarefaction (suction predation).

### *Experimental procedure*

When transferring fish from the holding tanks to the experimental chambers, care was taken so as not to harm them or cause much distress. The fish was herded into glass containers, and thus never left the water while the experimental chamber was always prepared in advance so that there would be as little activity as possible in the experimental room after the transfer of the fish. This left only the fitting of the lid and making sure all air was removed from the chamber in question. The number of fish in the chamber during experiments differed between species, 1-2 for sprat in both setups and 10 for diploid and triploid salmon fry in the swing chamber. As explained earlier under water preparations, the temperature, pressure and salinity for the experiments were kept nearly identical to the conditions in the fish holding tanks, so as to reduce the acclimatization period needed. The acclimatization period varied between species and individuals from 2-12 hours. The criteria for initializing experiments were that the fish exhibited a calm behaviour where they did not swim against the walls or performed sporadic changes in direction. The lighting in the experimental rooms were dimmed and an IR laser was used as extra light under high speed video takes. Stimulation order were randomized using the web site <http://www.randomizer.org/>, and a intervals between stimulations were 5 minutes if no behavioural response was observed, 10 minutes if a behavioural change was observed and 15 minutes if a startle response were observed.

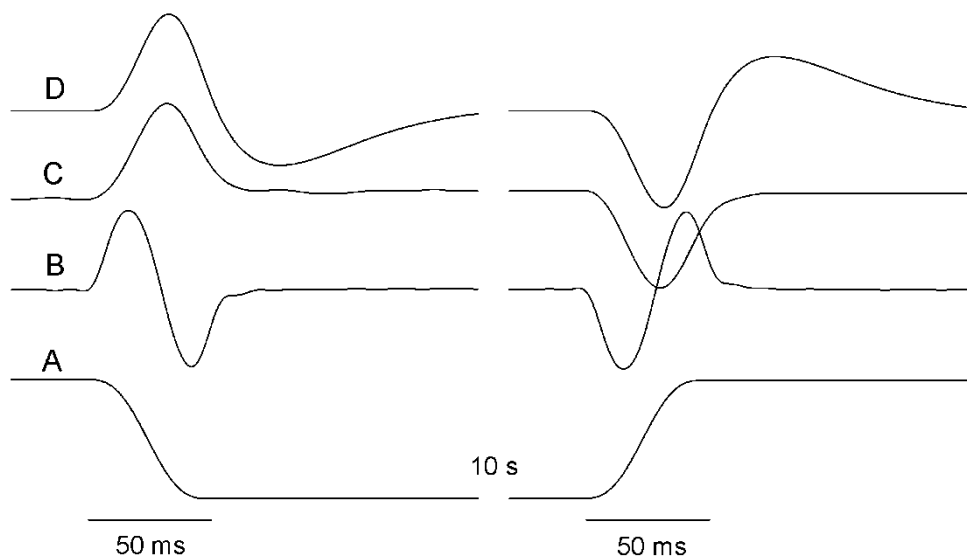


**Figure 2.10.** Stimulus waveforms recorded for the experimental pressure chamber system when operated in pressure mode at 20 Hz. All recorded waveforms were unfiltered by the recording equipment in order to prevent stimulus waveform distortions. (A) The specially designed driving voltage waveform to the vibrator consisted of two single cycle and ramp shifted sinusoidal voltages following the equation  $\pm (\omega t - \sin \omega t)$ , and separated in time by 10 s. (B) The particle acceleration in the pressure chamber as measured by accelerometers attached to vibrator pistons (see Figure 2.6). The acceleration waveform closely approximated a transient free and single frequency (20 Hz) sinusoidal waveform. (C) Pressure waveform measured in the centre of the test chamber by the Reson hydrophone, i.e. without pre-amplification and filtering. The transient free pressure increase (compression) created closely approximated a 20 Hz sinusoidal waveform d.c. shifted one peak value and phase shifted to start at  $-90^\circ$ . (D) Pressure waveform measured in the centre of the test chamber by the highly sensitive Sensor hydrophone. The differential pre-amplification and low pass filtering of this hydrophone induced distortions in recorded pressure waveform. However, peak pressure values measured by the two hydrophones differed by less than 4 dB in all stimulations employed.

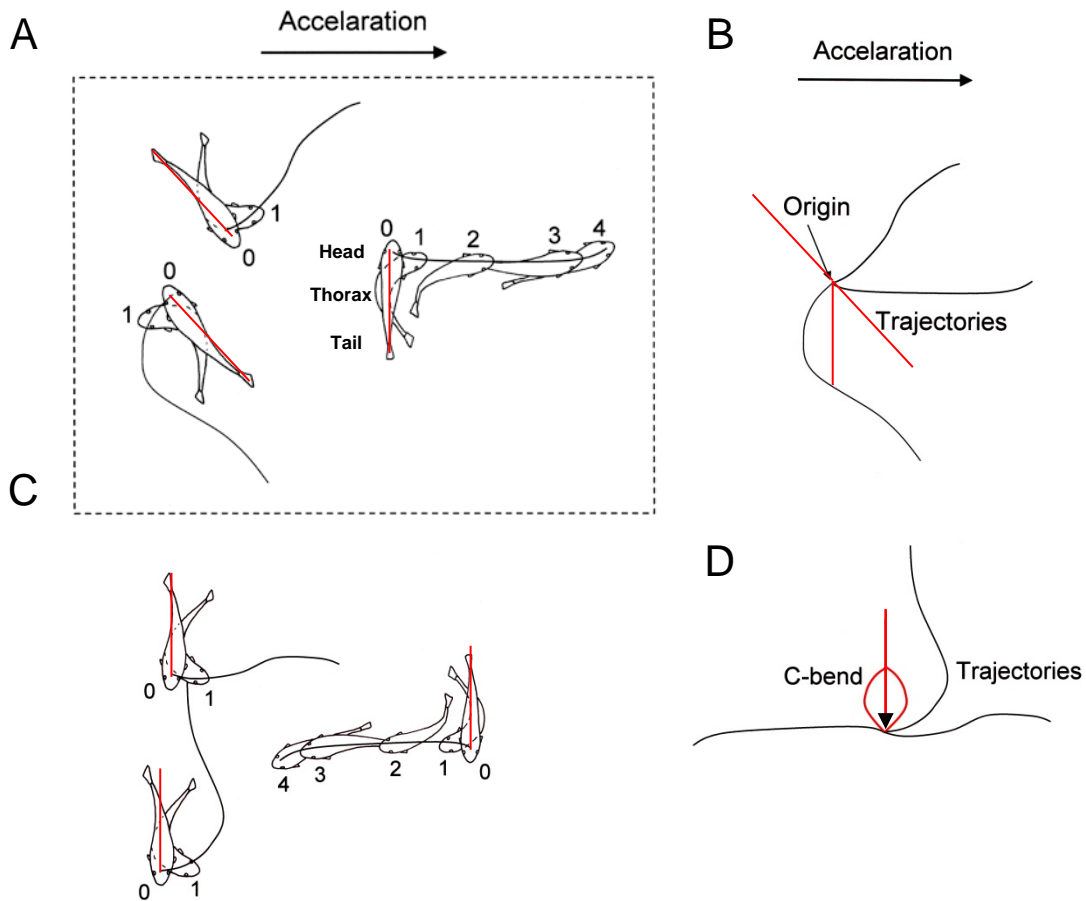


**Figure 2.11.** Methods used to present the C-response trajectory plots for sprat and salmon fry in the two experimental chambers. (A) Initially the test chamber outline was traced along with the fish body. Finally the position of the head was traced frame by frame for 140 ms with reference to direction of the initial acceleration of the test chamber. (B) For clarity startle trajectories were plotted with all fish repositioned with the head in the origin. The initial orientation of the fish was not changed. (C) Alternatively startle trajectories were plotted with all fish reoriented to a head down position, as well as repositioned with the head in the origin (D). This was mainly done to clarify startle response turning angles. (Modified from sketches by H. E. Karlsen).

### *Video analysis and statistics*

Videos were imported to the video analysis program ImageJ where latency responses were measured as time from a LED light to the first frame where the fish starts its C-bend. The LED light received voltage from the analogue to digital converter so as to show the precise moment of stimuli start. When a C-response was confirmed we used an add-on for ImageJ called MTrackJ to trace the C-response trajectories in the video. Firstly, the four corners of the test chamber were traced, and a distance calibration line added for calibrations in a pixel to mm ratio. Then the tail, thorax and head of the fish was traced for frame 0 (LED on) in reference to the trace of the chamber before. Subsequently, the startle trajectory was determined by tracing the head and thorax positions frame by frame for the total startle duration of 140 ms (Figure 2.11). The coordinates were then imported to Microsoft Excel 2010 for management and analysis. In presentations, individual fish were either repositioned with the initial head position in the origin (Figure 2.11B), or fish were reoriented to an initial head down position before being repositioned with the initial head in the origin (Figure 2.11D).

The statistical analyses employed were Students t-tests and Mann-Whitney Rank Sum tests for group comparisons. This was done in Sigmaplott version 11 and Systat Version 13 (Systat Software Inc, USA). Binomial logistic regressions in order to compare startle response probabilities were performed in Systat 13. Directionality of startle response trajectories were examined by Mardia-Watson-Wheeler tests for equal directional distributions and Rayleigh's R for uniform directional distributions using Past 3.02. The chi square tests were performed in Excel.

### 3. Results

#### *Startle response probabilities in sprat in the pressure and the swing systems*

Initially, acoustic startle behaviour in sprat was studied in the experimental pressure chamber set-up operated in pressure and displacement mode. The stimulus waveforms employed closely approximated a 20 Hz single cycle sinusoid of particle acceleration and compression or particle acceleration and rarefaction (see Methods, Figure 2.10). The number of fish examined and startle responses accepted, i.e. which occurred within the area of interests and with a latency of less than 60 ms, is presented in Table 1 in the appendix. In pressure mode operation, the sprat readily performed typical startle behaviours with the defining initial C-bend of the body followed by a short duration (approximately 140 ms) escape movement. However, a binomial logistic regression run on the pressure phase and level (Figure 3.1A) showed significantly ( $p < 0,001$ ) higher probability for a startle response to occur during exposure to a compression pulse than to a rarefaction pulse in the pressure system. The probability for startle behaviour was about 0,2 at a compression level of approximately 120 dB re 1  $\mu$ Pa, but this tentative acoustic startle threshold level was not examined in detail. A probability close to 1 for startle behaviour was observed at a

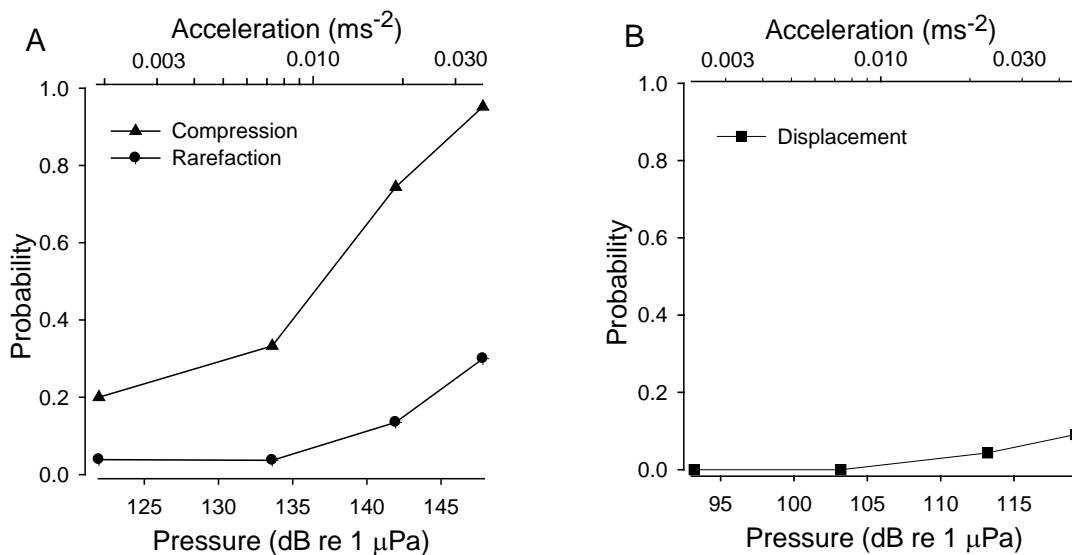


**Figure 3.1.** (A) Probabilities for sprat performing startle behaviour (C-response) when exposed to different levels of particle acceleration associated with compression versus particle acceleration associated with rarefaction during pressure mode operation of the pressure chamber. (B) Probabilities for startle behaviour in the sprat when operation of the pressure chamber was switched to displacement mode. Levels of particle acceleration were the same as in (A) but the associated pressure levels were significantly reduced.

compression level of about 147 dB re 1  $\mu$ Pa and a particle acceleration of about  $3,5 \cdot 10^{-2} \text{ ms}^{-2}$ . In displacement mode, operation of the pressure chamber set-up, the sprat were largely unresponsive (Fig. 3.1B). In displacement mode the electromagnetic vibrators operated in a push and pull mode, and as a consequence the ratio of particle acceleration to pressure was greatly increased within the pressure chamber compared to pressure mode operation (see Methods, Fig. 2.8). At the highest intensity examined in displacement mode, a compression waveform largely comparable in shape to the one produced in pressure mode operation could be recorded at a level of approximately 119 dB re 1  $\mu$ Pa. The associated particle acceleration level was approximately  $3,6 \cdot 10^{-2} \text{ ms}^{-2}$ . Still the probability for startle behaviour was very low and in the area of 0,1. Thus, it was clear that startle responses observed in sprat in pressure mode operation were triggered and driven mainly by the acoustic pressure component of the stimulus.

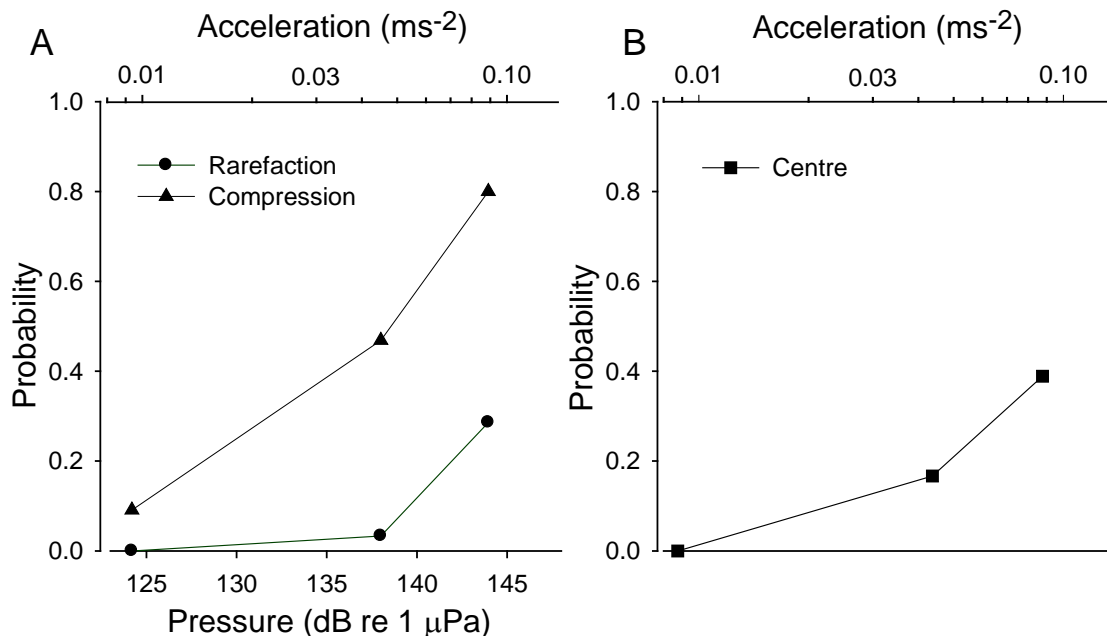


**Figure 3.2** (A) Probabilities in sprat for startle behaviour (C-response) to occur in the lagging half (compression) and leading half (rarefaction) of the experimental swing chamber. The probability differences between the two pressure phases were highly significant. (B) Probabilities for startle behaviour in the centre of the swing chamber. These were not significantly different from the rarefaction probabilities.

As for the pressure chamber, the stimulus waveforms obtained in the experimental swing chamber closely approximated a 20 Hz single cycle sinusoid pulse of particle acceleration associated with initial compression (lagging half of the swing chamber), with initial rarefaction (leading half) or with no significant initial pressure changes (centre of the swing chamber). There was a significantly higher probability for sprat to perform startle behaviour in the compression half of the swing chamber compared to the rarefaction half



(Figure 3.2A). For both compression and rarefaction stimulation the startle response probability curves from the pressure and swing chamber matched for pressure levels but not for acceleration levels. This further indicates that the behaviours were triggered by pressure and not particle acceleration. The different variables of pressure phase and level were examined by performing a two-way binomial logistic regression with the probabilities for a startle response at intermediate intensity in the lagging end of the chamber as a baseline. There was no significant difference between the C-response probabilities for sprat in the centre and lagging end of the system ( $p = 0,157$ ), while changing the stimulus level or the position of the sprat to the leading end of the system gave a significantly different startle response probability ( $p < 0,05$ ).

#### *Startle response latencies in sprat in the pressure and the swing system*

A high speed video camera with a frame rate of 500-1000 frames/s is necessary for accurate measurements of startle response latencies. Such a camera was available only late in the experiments performed on sprat. In the pressure system startle response latencies were measured at 1000 Hz video frame rate for 7 sprat at 133 dB re 1  $\mu$ Pa and 10 sprat at 142 dB re 1  $\mu$ Pa. The mean  $\pm$  S.D. response latencies were  $29,3 \pm 8,7$  ms and  $39,1 \pm 7,1$  ms, respectively. The difference was significant (t-test,  $p = 0,026$ ). In the swing system, startle response latencies were measured for 11 sprat at approximately 138 and 144 dB re 1  $\mu$ Pa. The mean  $\pm$  S.D. response latencies were  $30,6 \pm 11,8$  ms and  $38,8 \pm 12,6$  ms and not significantly different (Mann-Whitney U test,  $p = 0,132$ ). When referred to pressure level, startle response latencies observed in the pressure system and the swing system appeared to be comparable.

#### *Startle response directionality in sprat in the pressure and the swing system.*

The large majority of the recorded startle responses in sprat were elicited by compression in the pressure and in the swing system. Startle response trajectories and directionality were examined for these responses only. Startle trajectories, covering 0-140 ms, for sprat in the pressure chamber are shown in Figure 3.3A. In the figure all fish were rotated to

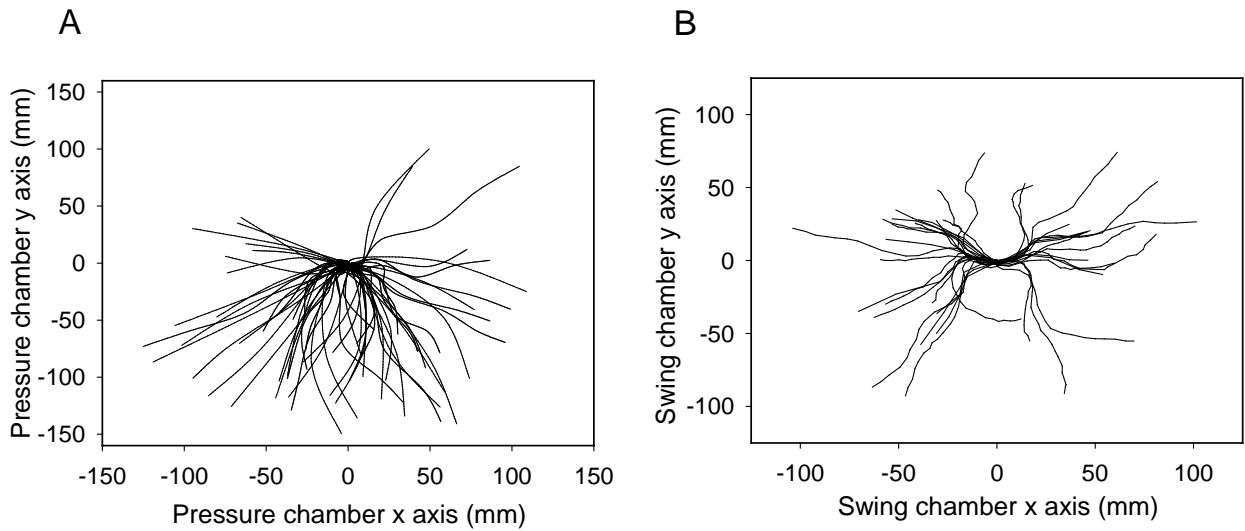


**Figure 3.3.** (A) Startle response trajectories, covering 0-140 ms, in sprat elicited by compression in the pressure chamber. (B) Startle trajectories in sprat elicited by compression in the swing chamber. All test fish have been vertically orientated with head down and repositioned with the head in the origin.

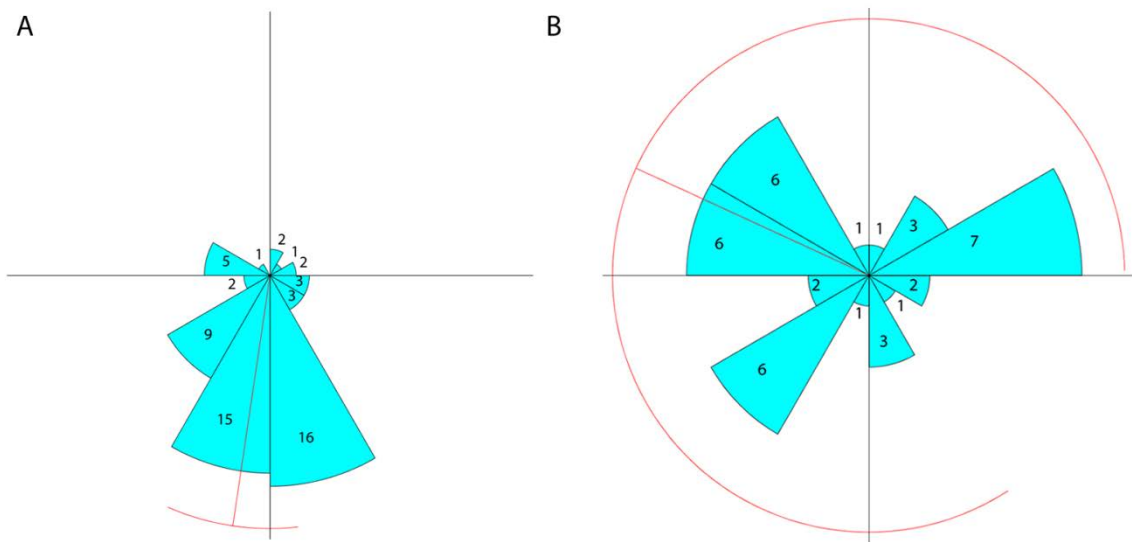


**Figure 3.4.** (A) Startle response turning angles (see main text) in sprat, all reoriented to a vertical head down position, in the pressure system (A) and in the swing system (B). The red line represents the mean  $\pm$  S.D. of the final startle response direction, i.e. the straight line connecting initial and final head position. In the pressure system most startle response turning angles fell within 30 degrees to the left or to the right of the initial orientation of the fish, and they were significantly different from that of a uniform distribution (Rayleigh's R for uniform distribution,  $p = 0,70$ ). In the swing chamber startle response turning angles were more varied than in the pressure chamber and not significantly different a uniform distribution (Rayleigh's R for uniform distribution,  $p < 0,001$ ).

a vertical head down orientation and repositioned with the head in the origin. The number of sprat in the pressure system that had an initial right turn was 30, while 34 had an initial left turn. These observed directional changes did not differ significantly from an expected 50-50 distribution (chi-square,  $p = 0,617$ ). In the swing system, 22 sprats had an initial right turn and 18 had an initial left turn, again not significantly different from a 50-50 distribution (chi-squared,  $p = 0,527$ ). The trajectory lengths differed significantly (t-test,  $p < 0,001$ ) with means of  $109 \pm 27$  mm for the pressure system and  $76 \pm 24$  mm for the swing system. The distribution of startle response turning angles, i.e. the angle between the initial orientation of the fish and the straight line connecting the initial and final position of the head of the fish are shown in Figure 3.4. In the pressure system, the turning angle of most fish (52,5%) fell within a sector of 30 degrees to the left or to the right of the initial orientation of the fish, and differs significantly from a uniform distribution (Rayleigh's R for uniform distribution,  $p < 0,001$ ). In the swing chamber, startle response turning angles observed in sprat in the swing chamber were more varied than those observed in the pressure chamber, and they were not significantly different from a uniform distribution (Rayleigh's R for uniform distribution,  $p = 0,70$ ). The turning angles for both swing and pressure systems did not have equal distributions (Mardia-Watson-Wheeler test for equal distributions,  $P = 1,3 \cdot 10^{-5}$ ). Thus, a factor influenced startle response directionality in a significantly different way in the pressure system compared to the swing system.

In order to examine whether the difference in startle response directionalities and turning angles in sprat in the pressure and swing systems was due to higher levels of particle accelerations in the swing system, startle trajectories were plotted for the same direction of initial acceleration in the swing system (Figure 3.5). In the pressure system, the initial orientation of the sprat, i.e. immediately prior to startle behaviour, essentially covered all directions (Figure 3.5A). The same was true for the corresponding startle response trajectories (Figure 3.5C). When the sprat in pressure chamber was left in their initial orientations, the distribution of the turning angle directions (Figure 3.6A) was not significantly different from a uniform distribution (Rayleigh's R for uniform distribution,  $p = 0,52$ ). Thus, the fish performed basic startle responses which were unaffected by any strong unidirectional cues. For the swing system, the initial orientations and startle response trajectories which occurred when the swing chamber was accelerated from right to left, were flipped 180° horizontally. Thus, initial orientations of the sprat in the swing chamber were plotted as

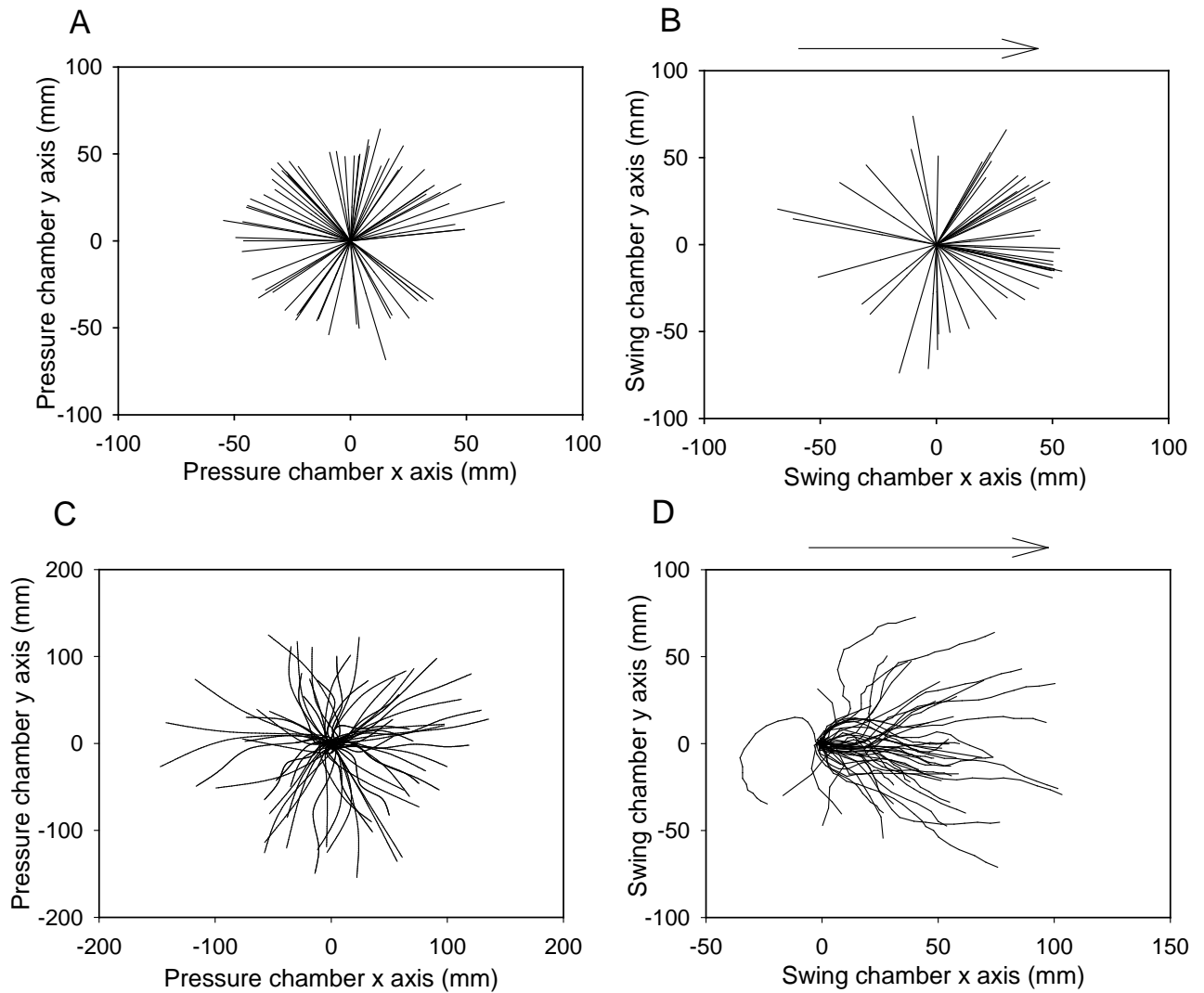


**Figure 3.5.** (A) The initial body orientation of sprat which performed an acoustic startle response when stimulated by a compression pulse in the pressure system. All fish were repositioned with the head in the origin. (B) The initial body orientation of sprat which performed a startle response when stimulated by a compression pulse in the swing system. Fish were repositioned with the head in the origin, and orientations of fish stimulated by initial acceleration to the left were flipped 180° horizontally to the right. Stimulations in the swing chamber thus depicted with initial acceleration to the right, as indicated by the arrow above the figures. The corresponding startle response trajectories observed in the pressure and the swing chamber are shown in (C) and in (D), respectively. There was a dramatic difference in the directionality of the startle responses in the two systems.

if all initial accelerations of the swing chamber occurred from left to right (Fig. 3.5B). The corresponding startle response trajectories observed in sprat in the swing chamber showed a strong directionality, and was significantly different from a uniform distribution (Rayleigh's  $R$  for uniform distribution,  $p < 0,001$ ). The two had significantly unequal distributions (Mardia-Watson-Wheeler test for equal distributions,  $P = 2,23 \cdot 10^{-6}$ ). Startle responses overall

occurred in the same direction as the initial acceleration (Figs. 3.5D and 3.6B). This strongly indicates that startle responses by sprat in the swing chamber were triggered by the pressure component of the stimulus, and that particle acceleration or the kinetic component of the stimulus provided response directionality. For the pressure system startle responses were triggered by pressure, but particle accelerations in this set-up did not appear to affect the behaviour significantly.

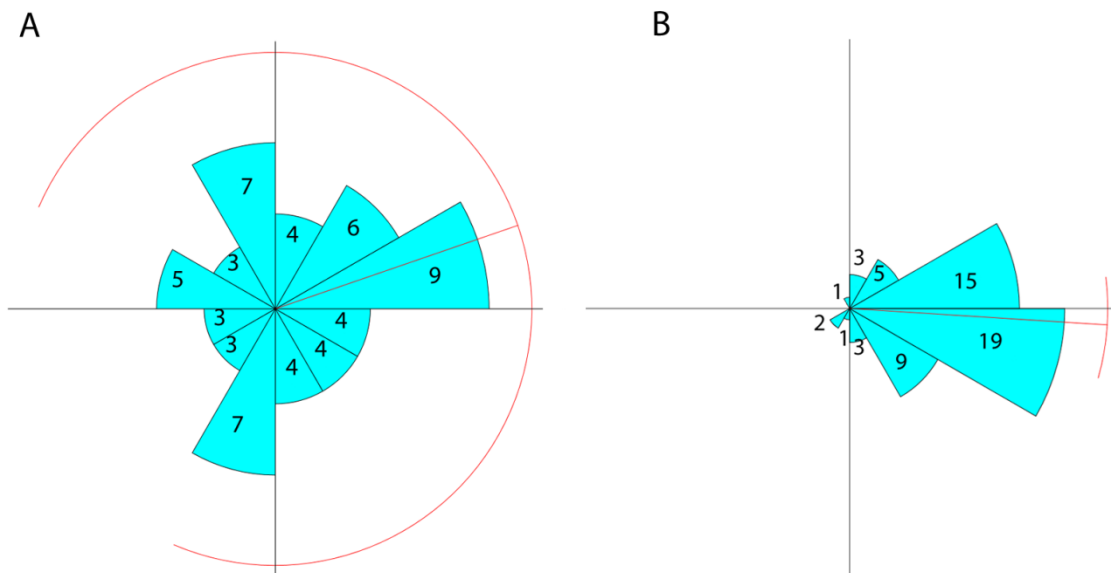


**Figure 3.6.** Startle response directions, i.e. the direction of the straight line connecting the initial and final fish head position, grouped in 30° sectors. (A) Startle directions observed in the pressure system. (B) Startle directions observed in the swing system when the initial chamber acceleration was from left to right.

*Startle responses probabilities in triploid and diploid salmon fry in the swing system.*

Both diploid and triploid salmon fry showed a distinct and typical startle behaviour when stimulated in the experimental swing chamber set-up. However, threshold pressure and particle acceleration levels for eliciting the behaviour responses were approximately 30 dB, corresponding to a factor of 32 higher than for the sprat, a fish hearing specialist. In addition, it was found that startle behaviour in diploid and triploid salmon were elicited with comparable probabilities in the leading, lagging and centre portions of the swing chamber (Figure 3.7). This strongly indicated that startle responses in the examined salmon were triggered by particle accelerations and not pressure. Thus, startle response probability in salmon was much less, if at all, influenced by pressure phase than in sprat.

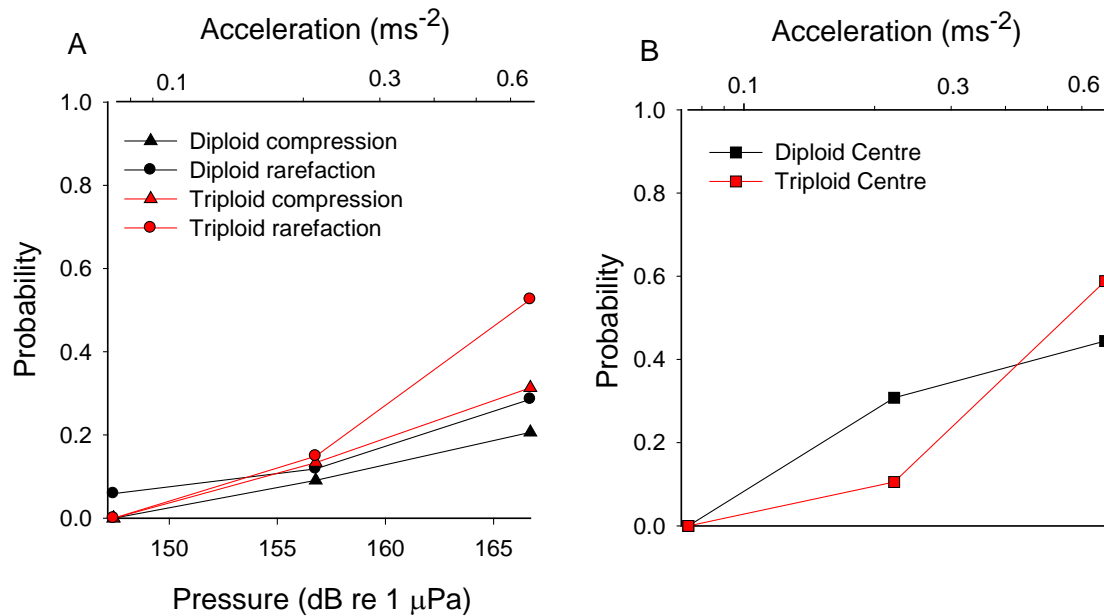


**Figure 3.7.** (A) Probabilities for eliciting startle behaviour in diploid and triploid salmon fry in the lagging (compression) and leading (rarefaction) half of the swing chamber. (B) Probabilities for eliciting startle behaviour in diploid and triploid salmon fry in the centre of the swing chamber.

A three-way binominal logistic regression model was examined with the startle response probability values for diploid salmon during stimulation by compression at the lowest intensity as baseline. The model showed a significant effect of all the independent variables including ploidy, pressure phase and stimulus level, but the odds ratio showed that the effect-size of ploidy and pressure phase were minor. Changing the ploidy of salmon from diploid to triploid gave a 60 % odds increase for a startle response while changing the stimulus intensity from low to high gave an 8944 % odds increase. Changing the pressure phase from compression to rarefaction or the pressure equalized centre gave an odds increase for a startle response of 79 % and 182 %. Explained in the form of Nagelkerke pseudo root squared; the ploidy, pressure phase and intensity explained 0,6 %, 1,9 % and 14,6 % of the deviance in the data respectively. Thus, the significant effect of ploidy and pressure phase on startle response probability should be interpreted with caution.

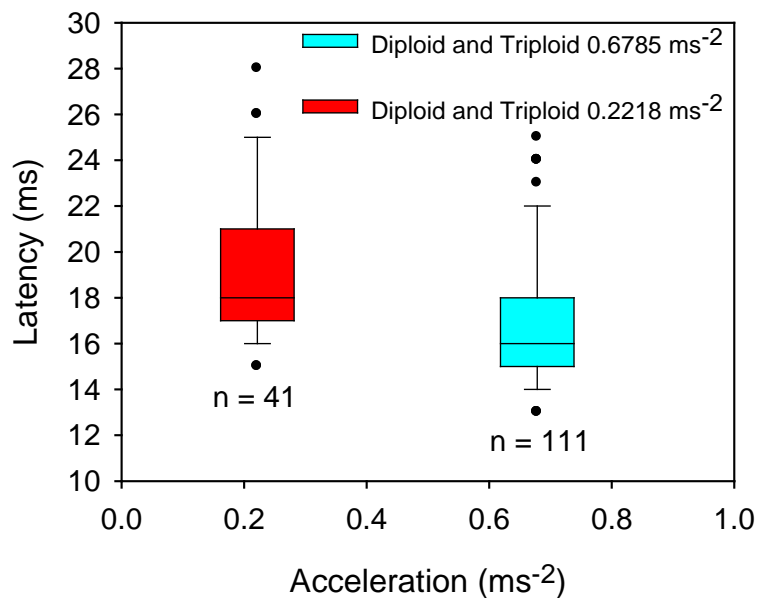


**Figure 3.8.** Boxplots of the latency times for diploid and triploid salmon fry for the accelerations  $0,22 \text{ ms}^{-2}$  and  $0,68 \text{ ms}^{-2}$  in the swing system. The horizontal line in the box represents the median value, while the area of the box above and below this line represents the upper and lower quartile with whiskers represent any variability outside.

*Startle responses latencies in triploid and diploid salmon fry in the swing system*

Mean startle response latency for diploid and triploid salmon when accelerated by  $0,68 \text{ ms}^{-2}$  was  $16,70 \pm 2,75 \text{ ms}$  and  $17,33 \pm 2,96 \text{ ms}$  was not normally distributed and their median values was not significantly different (Mann-Whitney rank sum test,  $p = 0,135$ ). The mean startle response latency time for diploid and triploid salmon for the intensity  $0,22 \text{ ms}^{-2}$  was  $18,50 \pm 2,41 \text{ ms}$  and  $20,70 \pm 3,99 \text{ ms}$ , was not normally distributed, and their median values was not significantly different (Mann-Whitney rank sum test,  $p = 1,20$ ). The mean values for both diploid and triploid salmon startle response latencies for stimulations with the intensities  $0,68 \text{ ms}^{-2}$  and  $0,22 \text{ ms}^{-2}$  respectively, was  $17,12 \pm 2,89 \text{ ms}$  and  $19,41 \pm 3,30 \text{ ms}$  respectively. It was not normally distributed, and their median values (Figure 3.8) differed significantly (Mann-Whitney rank sum test,  $p < 0,001$ ).

*Startle response trajectories for diploid and triploid salmon in the swing system*

Both diploid and triploid salmon performed startle responses in all the areas of the swing system lasting about 140 ms. The trajectories are plotted in Figure 3.9 with all fish oriented head down and in the same origin. The mean  $\pm$  S.D. startle response distance for diploid

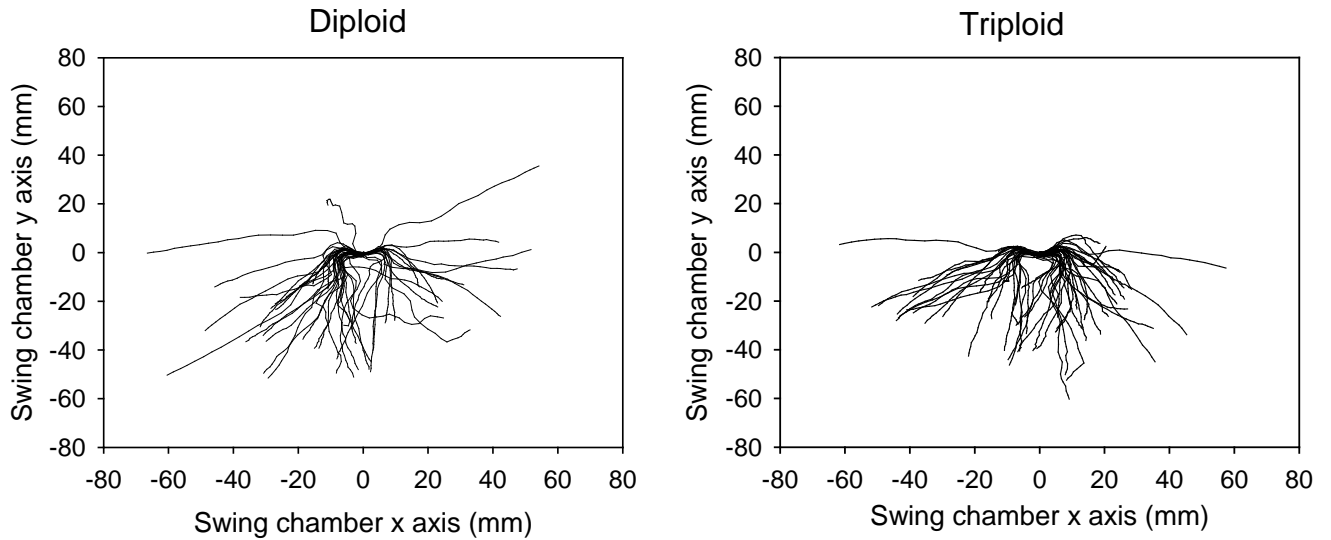


**Figure 3.9.** Diploid and triploid salmon fry startle response trajectories from 0-140 ms for all areas of the swing chamber. The plots are rotated so that all fish are oriented vertically with the head in the origin.

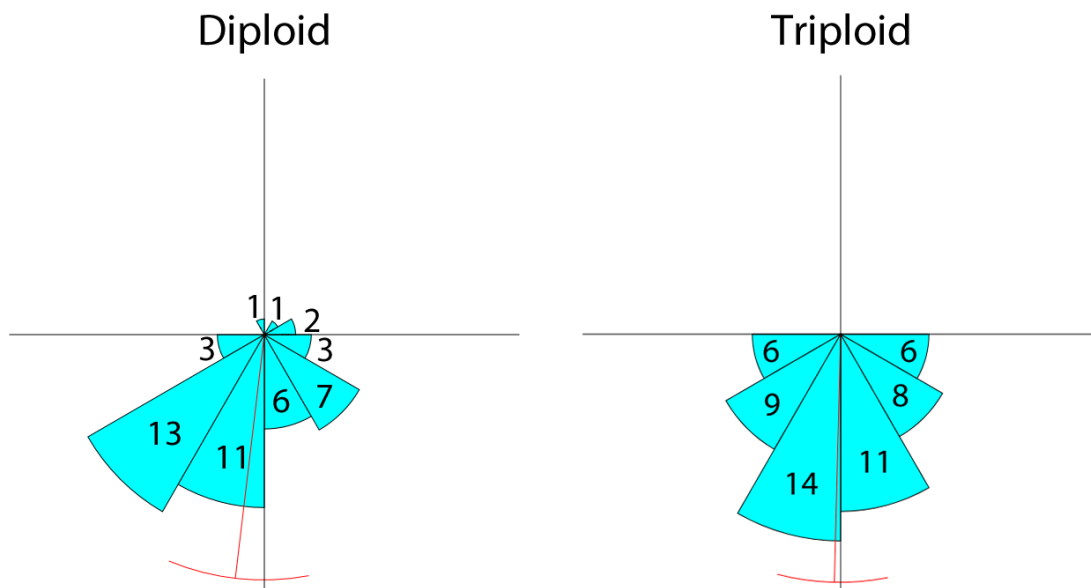


**Figure 3.10.** Final startle response turning angles, i.e. the angle between the initial fish orientation and a straight line connecting the initial and final fish head position, grouped in 30° sectors. The red line represents the mean  $\pm$  S.D. of the final startle response direction. All fish were reoriented head down and repositioned with the head in the origin for clarity.

and triploid salmon were  $49,65 \pm 13,92$  mm and  $46,17 \pm 11,79$  mm, respectively, and the difference was not significant (t-test,  $p = 0,270$ ). The number of diploid salmon that had an initial startle response to the right was 31 while 17 showed an initial direction to the left,



which is significantly different from an assumed 50-50 distribution (chi-square,  $p = 0,043$ ). For triploid salmon the corresponding distribution was 27 initial right and 32 initial left turns, which did not differ significantly from an assumed 50-50 distribution (chi square,  $p = 0,515$ ). The initial trajectories point outwards to each side in the initial phase but the final turning angles were mainly below  $90^\circ$  (Figure 3.10) and of the trajectories in general had a forwardly direction for both diploid and triploid fry with a relatively small deviation. There was no significant uniformity of the turning angles for diploid (Rayleigh's R for uniform distribution,  $p < 0,001$ ) and triploid salmon (Rayleigh's R for uniform distribution,  $p < 0,001$ ), and their distributions did not differ significantly from each other (Mardia-Watson-Wheeler test for equal distributions,  $p = 0.34277$ ).

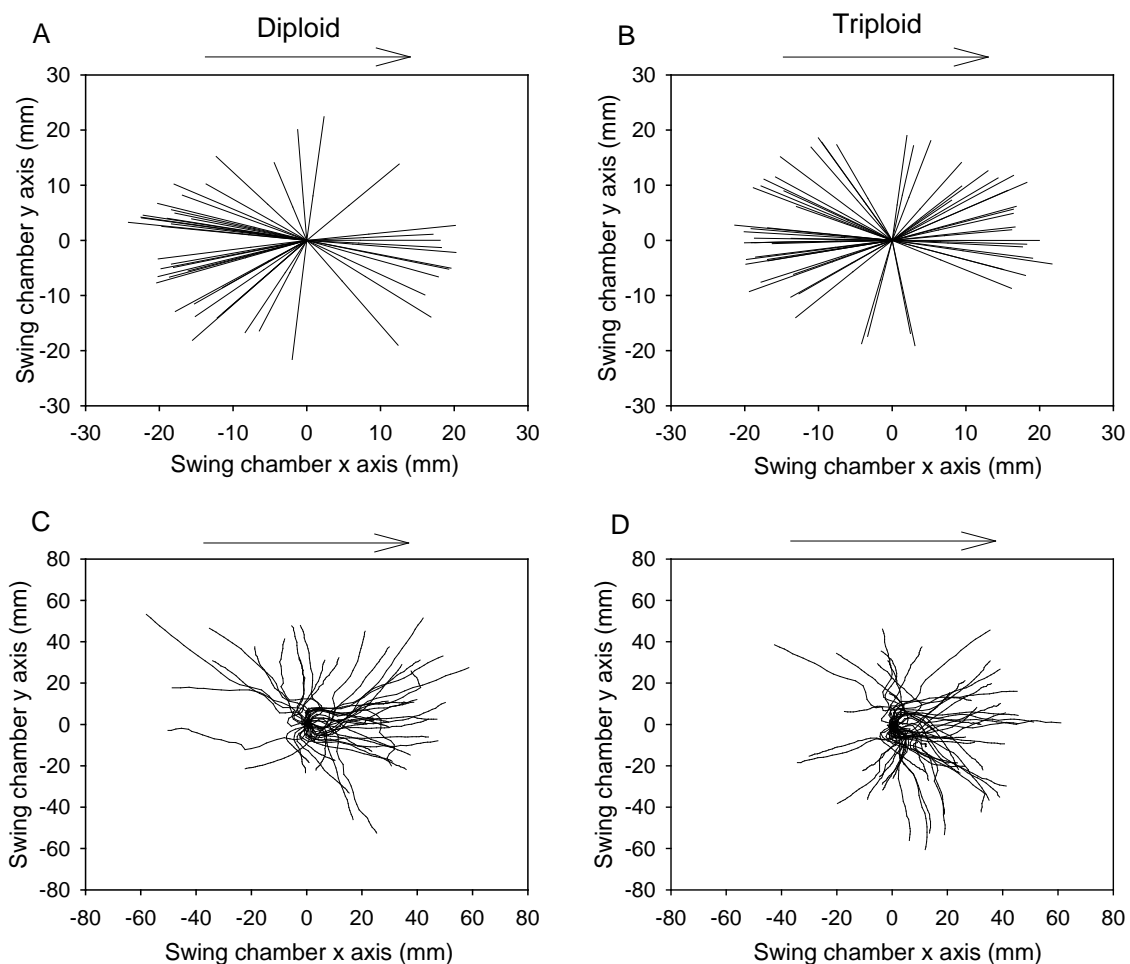


**Figure 3.11.** Diploid (C) and triploid (D) salmon fry C-response trajectories from 0-140 ms for all areas of the swing chamber with initial orientations (A and B). The initial orientations and C-response trajectories stimulated from right to left have been flipped  $180^\circ$  horizontally to depict acceleration in the same direction.

The initial orientation of diploid and triploid salmon prior to a startle response is illustrated in Figure 3.11A and B, with all initial orientations during initial acceleration to the left flipped 180° horizontally. This was done in order to display all startle trajectories for a single direction of initial acceleration, shown by the arrows in the figure. Salmon fry were initially both facing and oriented away from the direction of initial acceleration. The trajectories for diploid (C) and triploid (D) salmon showed a mean startle direction in the same direction as the acceleration (Figure 3.12). The distribution of startle response turning angles for diploid and triploid salmon with respect to the initial acceleration was significantly different from that of a uniform distribution (Rayleigh's R for uniform distribution,  $p < 0,001$ ), and the distributions are not significantly different (Mardia-Watson-Wheeler test for equal distributions  $p = 0.10155$ ). Overall triploid and diploid salmon fry startled in the direction of the initial acoustic particle acceleration.

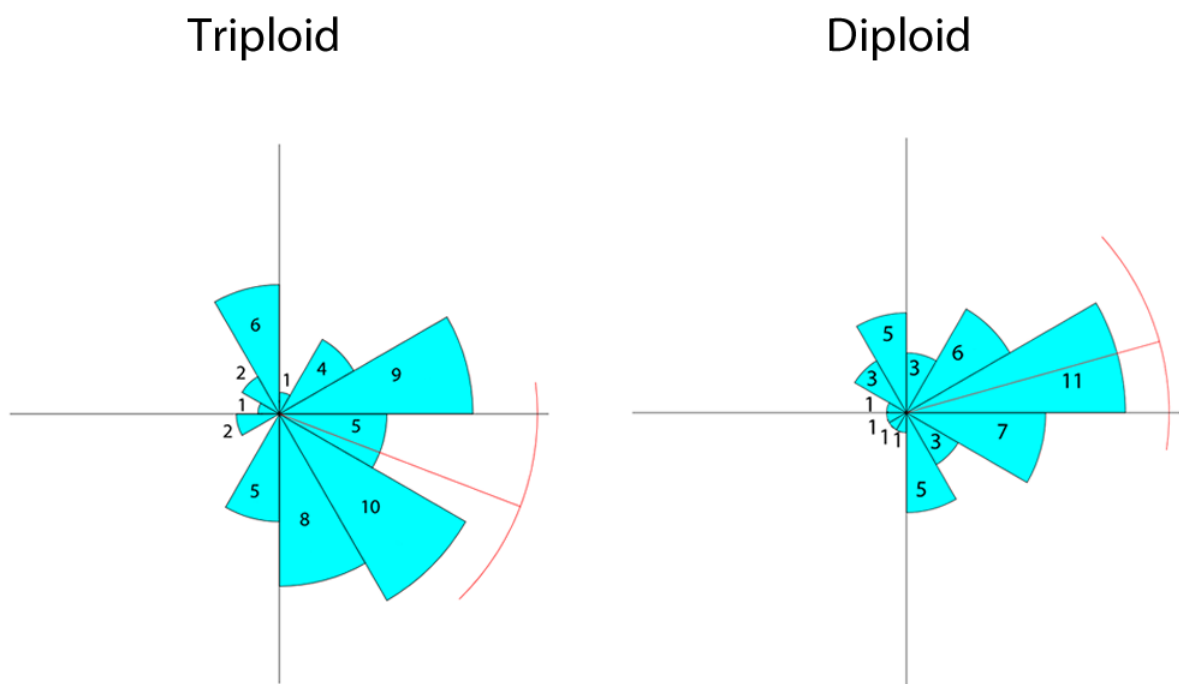


**Figure 3.12.** Turning angles for the diploid and triploid salmon fry C-response trajectories in the swing chamber (see Figure 3.11 C and D). It was measured as the angle between the direction of the initial acceleration and the straight line connecting the initial and final (after 140 ms) head position of the fish. Angles were grouped in 30° sectors. The red line represents the mean final startle response direction with respect to the direction of initial acceleration.

## 4. Discussion

### *Sensory information responsible for startle behaviours in the experimental setups*

Startle behaviours were readily triggered by the acoustic stimuli generated in the experimental swing and pressure systems in the examined sprat and the diploid and triploid salmon fry. Such responses in fish are initiated and driven by brain stem spinal neurons which are known to integrate direct neural input from a variety of sensory organs (reviewed by Faber et al., 1989; 1991; Korn and Faber, 1996; Zottoli and Faber, 2000; Eaton et al., 2001; Domenici, 2006; Medan and Preuss, 2014). In the present investigation they may thus have been influenced by several physical parameters.

Visual stimuli may trigger and influence startle behaviour (see Eaton and Emberley, 1991; Canfield, 2002; Domenici, 2006; Hanke, 2014). In the present study both the swing and the pressure system were surrounded by thin white curtains extending between the video camera, placed approximately 1 m above the test chambers and the transparent lids of the test chambers. The experimental fish were thus essentially surrounded by a homogenous visual field, and it was therefore unlikely that external visual cues affected the observed startle behaviours. This conclusion is supported by the findings that startle behaviours performed in the swing system by the sprat and salmon fry differed significantly in their threshold levels and adequate stimulus, and by the fact that startle behaviours performed by sprat in the pressure and swing system were consistent. If startle behaviours were dominated by external visual cues such as the minute displacements of the swing chamber during accelerations, the observed species differences in startle performance would be unlikely. In addition, ongoing experiments, not treated in this thesis, have been carried out on sprat in complete darkness using IR-cameras and lightning. These tests showed startle behaviours fully comparable to those elicited in the dim light conditions of this study (Karlsen, pers. med.).

Lateral line organs (neuromasts) have the same density as the surrounding water, and they are therefore not activated when the fish and surrounding water volume are accelerated as a unit. In contrast to the mass loaded otolith organs of the inner ear, neuromasts do not function as inertial motion detectors. Instead, the lateral line system in fish is designed to detect low frequency water movements and pressure gradients along the fish body (for extensive reviews see Bleckmann, 1993; Webb et al., 2007; Bleckmann and Zelick, 2009; Bleckmann and Mogdans, 2014). Lateral line stimulation, especially, in the tail and head region, may trigger startle behaviour in fish (Faber and Korn, 1975; Korn and Faber, 1975;

Mirjany and Faber, 2011; Mirjany et al., 2011) and as for visual stimuli, stimulating the lateral line system may modify startle behaviour (Gray, 1984; Canfield and Rose, 1996; Mirjany et al., 2011). The swing system was specifically designed to accelerate the experimental fish and the surrounding water together as a unit, and thus to not cause relative movements between external water and the experimental fish. In addition, the areas of interest in the test chamber ensured that startle behaviours recorded occurred in fish with a distance of more than one body length from the side walls of the test chamber. This is generally considered to be beyond limits of the distance touch ability of the lateral line system, i.e. the detection of distortions, caused by nearby objects, in the flow field surrounding a swimming fish (see Bleckmann and Zelick, 2009; Bleckmann and Mogdans, 2014).

A key characteristic of clupeid fish is the presence of a subcerebral perilymphatic (extracellular fluid filled) canal which crosses the head between the lateral lines. This fluid canal structure, named the *recessus lateralis*, runs from the lateral line canal just behind the eye on one side of the fish, underneath the brain, and to the lateral line canal just behind the eye on the opposite side of the fish. In sprat and herring it has been shown that lateral line canal organs just behind and underneath the eyes are extra sensitive and activated by tiny pressure gradients applied across the head of the fish, causing fluid displacements in the *recessus lateralis* canal, with thresholds in the range of 2-5 Pa/m (see Denton and Gray, 1993). This is below the estimated maximum linear pressure gradient across the 54 cm internal length axis of the swing system of 3,7 -37 Pa/m for the pressure range 120 -140 dB re 1  $\mu$ Pa. Typically, the pressure gradient sensitive head lateral line canal organs in clupeids are activated by self-generated pressures produced by lateral movements of the head. These pressures are equal and opposite in sign on the left and right sides of the head, and oppose the self-generated accelerations that produce them (Denton and Gray, 1993). In contrast, when sprat and surrounding water were accelerated together in the swing and the pressure system, the net pressure gradient needed to activate lateral line organs would be minimal and so would any flows through the *recessus lateralis* canal. Thus, even though clupeids have head lateral line canal organs sensitive to minute pressure gradients, this sensory system will not be activated to any significant degree in the swing system. The same line of reasoning holds true for superficial and canal neuromasts of the salmon. Therefore, it was very unlikely that the lateral line system affected the observed startle behaviours in sprat and salmon in the set-ups used.

In conclusion, acoustic startle behaviours observed in sprat were most likely elicited by pressure acting on the pressure sensitive bullae and inner ear utricle otolith system. This

would explain the fact that startle behaviour thresholds in sprat were consistent in the pressure and swing systems. The pressure system was designed to create homogeneous pressure waveforms within the pressure chamber when operated in pressure mode, and thus in this mode to generate negligible pressure gradients and thereby no activation of lateral line organs. Startle behaviours observed in the salmon fry were triggered with close to identical probability in the centre of the swing chamber (with very low initial pressure changes) compared to the lagging and leading halves with large compression and rarefaction, respectively. This suggests that startle behaviours in the salmon were triggered by acoustic particle accelerations acting on the inner ear otolith organs.

*Pressure phase sensitivity of startle behaviours in sprat and the evolution of acoustic pressure sensitivity in fish hearing specialists*

Acoustic startle behaviour in the clupeid fish hearing specialist sprat was found to be triggered by compression at significantly higher probabilities than for rarefaction in both the pressure system and the swing system. This was comparable to earlier findings in the Otophysan fish hearing specialist the roach in the swing system (Karlsen et al., 2004). Startle thresholds were in the range of 120 dB re 1  $\mu$ Pa in sprat in the pressure system operated in pressure mode as well as in the swing system. In terms of predator-prey interactions, this suggests that the behaviour has evolved in order to evade striking predatory attacks mainly compared to predatory attacks from suction type of predators. An acute sensitivity to the compressions created in front of a charging predator would give the prey fish maximum time to perform a successful startle escape. The specialized adaptations evolved in different fish orders for increased auditory pressure sensitivity are highly diverse (see Ladich and Popper, 2004; Braun and Grande, 2008; Popper and Ketten, 2008; Ladich, 2010; 2014). In carp fish, such as roach and others, they include a chain of small bones, the Weberian ossicles, which effectively transfer sound pressure induced by swim bladder volume pulsations to the saccule otoliths of the inner ears. In clupeid fish the specializations include forward swim bladder extensions which end in the specialized gas filled bullae located in close proximity to the inner ear utricle otoliths. In other groups such as the elephant fish (family Mormyridae, order Osteoglossiformes) the specializations include small gas filled structures, derived from the swim-bladder during embryonic development, closely associated with the inner ear saccule otolith. Clearly, adaptations for high pressure sensitivity have evolved independently several times in fish, and must have had a strong adaptive value. In carp fish it was found that

acoustic startle behaviour were triggered by compression pulses mainly as opposed to rarefaction pulses (Karlsen et al., 2004). The same was found for sprat in the present study, and the same has recently been documented in the pressure and in the swing system set-up for the Mormoridae species *Gnathonemus petersii* (Karlsen, pers med.). Thus, a unifying characteristic of fish hearing specialists appears to be acoustic startle behaviour triggered mainly by compression. This strongly suggests that the acute inner ear pressure sensitivity found in these fish have evolved as adaptations to detect low frequency pressures in the near field in order to evade attacks by striking predators. Predator-prey interactions may thus have been the decisive driving force in the independent evolution of the various peripheral mechanisms for pressure sensitivity and thereby enhancement of sound reception in fish.

Fish are highly vocal and produce sounds by twitching of specialized sonic muscles attached to gas-filled structures like swim bladders, by grinding of body structures and more (see Popper et al., 2003; Ladich, 2010; 2014). Many fish groups such as cod fish are known to produce species specific sounds of great importance during courtship and spawning. It has therefore been suggested that hearing refinements in fish have evolved for improved acoustic communication (see Braun and Grande, 2008; Ladich, 2014). The problem with this argument is that barely any species within the fish hearing specialist order Cypriniformes (carp fish) have been found to produce sound, and no sonic muscles have yet been documented. In addition, far from all sound producing fish are hearing specialists. Communication does thus not appear to be able to explain the evolution of hearing enhancements in fish.

It is well documented that fish hearing specialists detect high frequencies (a few kHz) far better than fish hearing non-specialists. Thus, adaptations for increased pressure sensitivity extend the auditory range. However, taken into account that biologically produced sounds are mainly of low frequency, well below 100 Hz, it seems unlikely that pressure sensitivity in fish originally evolved for increased high frequency sound detection. The importance of frequencies in the kHz range in fish hearing remains obscure.

#### *Startle responses directionality in sprat in the pressure and the swing system*

It has been proposed that acoustic pressure sensitivity evolved in fish hearing specialists as a means for directional hearing and sound source localization (see Braun and Grande, 2008; Popper and Ketten, 2008; Ladich, 2014). The argument is that a fish oscillating in a sound field will not be able to detect the location of a sound source based on inner ear detection of particle acceleration alone. There will be a 180° ambiguity. This ambiguity can

be resolved if fish were able to separately detect pressure phase since sound induced oscillation towards a sound source typically is associated with a pressure increase while oscillation away from a sound source is associated with a pressure decrease. Thus, by comparing particle acceleration and pressure phase, the fish will be able to decide the direction to a sound source. This is the basis for the so called phase theory for directional hearing and sound source localization in fish (Shuijf, 1975, 1981). There are very limited experimental data investigating the phase theory. However, both clupeid and carp fish are known to be highly pressure sensitive, and to have acoustic nerve fibres separately driven by compression and rarefaction (Piddington, 1972).

In the swing system, startle behaviour triggered by compression was highly directional and overall occurred in the direction of the initial acceleration. This is identical to the earlier finding for the carp species roach in the swing set-up (Karlsen et al., 2004). The results are in accordance with predictions of the phase theory for directional hearing in fish (Shuijf, 1975, 1981; Buwalda et al., 1983). However, the phase theory focuses on analyses of pressure phase and particle accelerations over several periods of a sound stimulus, i.e. analyses in the frequency domain. Contrary to this, the directionality of the startle behaviours observed in this study clearly occurred nearly instantly and in the time domain. Thus, with respect to acoustic startle behaviour and adaptive movements away from a threat, the question of directionality appears to be reduced to detecting and responding relative to the direction of the initial particle acceleration. Since the behaviour takes place in the near field with an increased ratio of particle accelerations to pressure compared to the far field, this would appear to be a natural mechanism. Thus, it may well be that the observed directionality of the startle behaviours in sprat was not based on pressure detection and analyses of pressure phase as suggested by the phase theory. This is supported by the fact that startle behaviours in salmon were highly directional in the swing system as well, even though this species is a fish hearing non-specialist and most likely insensitive to sound pressure. Like sprat, the salmon overall escaped in the direction of initial acceleration, and this occurred in the leading, the centre as well the lagging sections of the test chamber. It is thus concluded that startle response directionality in sprat and salmon fry in the swing system were based on initial particle acceleration detection by the directional sensitive inner otolith organs. In this respect, the apparent lack of directionality of sprat startle behaviours in the pressure system when operated in pressure mode may have been due to insufficient levels of particle accelerations.

The phase theory for directional hearing in fish has been extended to a neurological XNOR model for explaining and predicting startle response directionality by fish (Eaton et

al., 1995; Guzik et al., 1999; Casagrand et al., 1999). According to the XNOR model fish should interpret an experienced acceleration combined with compression as movement away from a sound source in the form of a striking predator, and thus startle by escaping in the same direction the fish is being accelerated. In addition, the model state that fish should interpret an experienced acceleration combined with rarefaction as movement towards a sound source in the form of a suction type of predator, and thus startle by escaping in the opposite direction the fish is being accelerated. The third prediction of the XNOR model is that fish will perform startle behaviour during compression and rarefaction with equal probability. The results of this study were not in accordance with the predictions of equal startle response probability during compression and rarefaction. The data obtained for startle directionality during rarefaction was too limited to say whether they were opposite to the direction of initial acceleration in a significant degree or not. As mentioned in the previous section, it is still an open question whether a neuronal pressure phase versus particle acceleration analyses is necessary to explain startle response directionality in fish. Thus it may be that the generally accepted neurological XNOR-model has no validity for fish hearing specialists.

#### *Acoustic startle response latencies in sprat*

Startle response latencies in sprat in the pressure system were about 29 ms and 39 ms for pressure levels of approximately 133 and 142 dB re 1  $\mu$ Pa, respectively, in the pressure chamber and about 31 ms and 39 ms for pressure levels of approximately 138 and 144 dB re 1 re 1  $\mu$ Pa, respectively, in the swing chamber. Thus, latencies were comparable in the two experimental set-ups with respect to pressure. Since the corresponding particle acceleration values in the pressure and swing system differed considerably, the consistence in startle response latencies with respect to pressure clearly indicated that startle behaviours in sprat were elicited by the pressure component and not by the acoustic particle acceleration component. In both diploid and triploid salmon fry startle response latencies in the range of 16-21 ms were found for stimulus levels of 0,22 – 0,66  $\text{ms}^{-2}$ , comparable to 158-166 dB re 1  $\mu$ Pa. The shorter response latencies in the salmon fry were clearly due to the difference in stimulus level. By extrapolating the values for sprat the expected startle response latency at 160 dB is about 14 ms. In fact, ongoing studies in the swing chamber set-up have found latencies at this level as low as 8-10 ms in sprat (Karlsen, pers med). It is thus clear that sprat



outperform the salmon fry studied. Sprat startle at approximately 30 dB lower acoustic pulse levels, in terms of pressure and particle acceleration, and their startle response latencies are shorter at high stimulus levels.

#### *Startle behaviour by diploid and triploid salmon fry in the swing system*

Both diploid and triploid salmon fry performed typical startle behaviours in response to acceleration in the swing system. Startle responses were performed in both the lagging half (compression), the centre (no initial pressure change) and the leading half (rarefaction) of the swing test chamber. Thus, the startle behaviour was triggered by acoustic particle acceleration, i.e. the kinetic sound component, and not by pressure as the situation was in sprat. Startle behaviour is a highly complex behaviour involving a sophisticated brainstem escape network as well as inner ear sensory organs and cells. Clearly, triploidy did not hamper this behaviour in the salmon fry. In fact a significant albeit marginal higher probability to perform startle behaviour was found in triploid versus diploid salmon. The effect of ploidy on the startle response probability explain 0,6 % of the total deviation in the data only. This was minor compared to stimulus level which explained 14,6 %.

Startle response latencies there were not significantly different in the two salmon groups, and both triploid and diploid salmon fry showed startle latencies in the range 16-21 ms for particle acceleration levels in the range 0,22 – 0,66 ms<sup>-2</sup>. In addition, triploid and diploid salmon were similar in showing the same significant effect of stimulus level on response latencies.

The directionality of startle responses were not significantly different between triploid and diploid salmon fry (see Figure 3.9 and 3.10), and both groups showed a clear directionality by overall performing startle responses in the direction of the initial acceleration irrespective of the initial body orientation (see Figure 3.11 and 3.12). Still, startle response turning angle with respect to the direction of initial acceleration were more limited in the salmon fry than in the sprat in the swing system. This is clear from a comparison of Figure 3.4B for sprat and Figure 3.10 for sprat. Thus sprat showed a significantly larger tendency to perform large startle turning angles (> 90°) in order to reach a final escape direction in line with the direction of the initial acceleration than the diploid and triploid salmon fry.

Startle duration and distance (and thereby maximum response velocities) did not significantly differ between triploid and diploid salmon fry. Startle response distance in diploid salmon were 49,65 ± 13,92 mm and in the triploid salmon 46,17 ± 11,79 mm,

respectively. The minor difference in mean values in the two groups was most likely linked to the minor difference in mean body length in the two groups of 19,7 mm in the diploid salmon and 18,3 mm in the triploid salmon. Startle response distance in terms of body length was 2,52 in both triploid and diploid salmon, which is exactly within the typical startle distance of 2-3 body lengths observed in fish (see Eaton et al., 1977; 2001).

The overall conclusion was that triploid and diploid salmon fry did not differ in their ability to perform acoustic startle behaviour. This was a somewhat unexpected finding given that triploidy significantly increases cell size and thereby may cause reduced cell numbers per tissue volume compared to diploid salmon (Swarup 1959, Small and Benfey 1987). In theory, this could affect acoustic startle behaviour in triploid salmon in a number of ways including functionality of the sensory hair cells, auditory nerve fibres, neurons of the brainstem escape and striated muscle cells. At present, the number of anatomical, physiological and behavioural studies of triploid salmon is very limited. However, a reduced mean muscle fibre length and /or reduction of fibres per unit area have been found in triploid salmonids when compared to diploids (Suresh and Sheehan 1998). Recently Fraser, Fjelldal et al. (2012) looked at the brain of pre-smolt Atlantic salmon, and found no difference in brain mass for diploids and triploids. There were, however, differences in the volume of different brain areas. The olfactory bulb was found to be reduced in triploids while the cerebellum and telencephalon was bigger in the triploids. At present there is just one behaviour study of triploid Atlantic salmon, and this found a reduced level of aggression compared to diploids (Carter et al., 1994). In addition, there is one study claiming to show a reduced responsiveness to acoustic and visual stimuli in triploid Ayu *Plecoglossus altivelis* (Aliah, Yamaoka et al. 1990). However, the acoustic stimuli in the study were undefined and crude, banging on the table carrying the fish and experimental aquarium, and behavioural response were simply recorded as increased swimming or not.

### *Conclusions*

Acoustic startle behaviours in the clupeid fish hearing specialist sprat were found to be elicited by a low frequency (20 Hz) acoustic pressure increase (compression) at threshold levels of about 120 dB re 1 $\mu$ Pa (amplitude, rms), i.e. by a stimulus mimicking key components in the acoustic signatures of a charging predator attack. Directionality of the startle behaviours was provided by acoustic particle acceleration, i.e. the kinetic sound component. Contrary to observations in sprat, acoustic startle behaviour in diploid and triploid salmon fry was elicited by acoustic particle acceleration, which in addition was responsible for directionality of the behaviour responses. There was no general difference in startle

behaviour by the triploid and diploid salmon. The concrete answers to the initial hypotheses addressed are given below:

**H01:** Acoustic startle behaviour is elicited with equal probability by sound pressure and by sound particle acceleration in sprat and triploid and diploid salmon fry.

Startle behaviour in sprat was found to be elicited by acoustic pressure rather than acoustic particle acceleration. Particle acceleration clearly provided directionality to the startle behaviours observed in the spring system, but the behaviours were triggered by the acoustic pressure component. The H01 must be rejected for this species.

Acoustic startle behaviour in diploid and triploid salmon fry was found to be elicited by particle acceleration, and to be essentially unaffected by pressure. Thus, the null-hypothesis was not rejected for this species.

**H02:** Acoustic startle behaviour is elicited with equal probability in sprat by acoustic compression, mimicking a charging predator attack, and by acoustic rarefaction, mimicking a suction predator attack.

There was a significantly increased probability for sprat to elicit a startle response as a consequence of an acoustic compression compared to an acoustic rarefaction. Therefore the null-hypothesis was rejected.

**H03:** Acoustic startle behaviours in diploid and triploid salmon do not differ with respect to their startle threshold level, startle latency, startle distance and startle directionality. Diploid and triploid salmon fry did not differ with respect to startle response latency, distance and directionality. However, the startle response probabilities were marginally increased in triploid salmon. Therefore the null-hypothesis was not rejected.

## Appendix

Stimulation	ms-2	db re 1 uPa	Size (n)	Responses	Mean
Compression	0.0369	147.8187	21	20	0.952
Compression	0.0188	141.9382	39	29	0.744
Compression	7.20E-03	133.6248	30	10	0.333
Compression	1.88E-03	121.9382	25	5	0.2
Rarefaction	0.0369	147.8187	20	6	0.3
Rarefaction	0.0188	141.9382	37	5	0.135
Rarefaction	7.20E-03	133.6248	27	1	0.037
Rarefaction	1.88E-03	121.9382	26	1	0.0385
Displacement	0.0457	119.2	33	3	0.0909
Displacement	0.0229	113.2	46	2	0.0435
Displacement	7.22E-03	103.2	45	0	0
Displacement	2.30E-03	93.2	23	0	0

Table 1. Number of sprat tested in the pressure system with stimulations, intensities and probabilities.

Stimulation	ms-2	db re 1 uPa	Size (n)	Responses	Mean
Compression	8.75E-03	124.19	11	1	0.0909
Compression	0.0437	138	32	15	0.469
Compression	0.0876	143.96	25	20	0.8
Centre	8.75E-03	60	12	0	0
Centre	0.0437	60	18	3	0.167
Centre	0.0876	60	18	7	0.389
Rarefaction	8.75E-03	124.19	11	0	0
Rarefaction	0.0437	138	30	1	0.0333
Rarefaction	0.0876	143.96	28	8	0.286

Table 2. Number of sprat tested in the swing system with stimulation area, intensities and probabilities.

Diploid	ms-2	db re 1 uPa	Size (n)	Responses	Mean
Compression	0.6785	166.7	63	13	0.20634921
Compression	0.2218	156.7758	77	7	0.09090909
Compression	0.0744	147.4148	27	0	0
Centre	0.6785	60	18	8	0.44444444
Centre	0.2218	60	26	8	0.30769231
Centre	0.0744	60	3	0	0
Rarefaction	0.6785	166.7	49	14	0.28571429
Rarefaction	0.2218	156.7758	76	9	0.11842105
Rarefaction	0.0744	147.4148	17	1	0.05882353

Table 3. Diploid salmon fry tested in the swing chamber with stimulation area, intensities and probabilities.

Triploid					
Stimulation	ms-2	db re 1 uPa	Size (n)	Responses	Mean
Compression	0.6785	166.7	67	21	0.31343284
Compression	0.2218	156.7758	60	8	0.13333333
Compression	0.0744	147.4148	43	0	0
Centre	0.6785	60	17	10	0.58823529
Centre	0.2218	60	19	2	0.10526316
Centre	0.0744	60	10	0	0
Rarefaction	0.6785	166.7	78	41	0.52564103
Rarefaction	0.2218	156.7758	47	7	0.14893617
Rarefaction	0.0744	147.4148	44	0	0

Table 4. Triploid salmon fry tested in the swing chamber with stimulation area, intensities and probabilities.

## References

- Aliah, R. S., Yamaoka, K., Inada, Y. and Taniguchi, N. (1990). Effects of triploidy on tissue structure of some organs in ayu. *Nippon Suisan Gakkaishi* 56(4): 569-575.
- Allen, J. M. and Blaxter, J. H. S. (1976). The functional anatomy and development of the swimbladder-inner ear-lateral line system in herring and sprat. *J. Mar. Biol. Ass. U.K.* 56: 471-486.
- Benfey, T. J. and Sutterlin, A. M. (1984): The haematology of triploid landlocked Atlantic salmon, *Salmo solar* L. *J. Fish Biol.* 24:333-338.
- Best, A. C. G. and Gray, J. A. B. (1980). Morphology of the utricular recess in the sprat. *J. Mar. Biol. Ass. U.K.* 60:703-715.
- Blaxter, J. H. S. and Denton, E. J. (1976). Function of the swimbladder-inner ear-lateral line system of herring in the young stages. *J. Mar. Biol. Ass. U.K.* 56:487-502.
- Blaxter, J. H. S. and Hoss, D. E. (1981). Startle response in herring: the effect of sound stimulus frequency, size of fish and selective interference with the acoustico-lateralis system. *J. Mar. Biol. Ass. U.K.* 61:871-897.
- Blaxter, J. H. S., Denton, E. J. and Gray, J. A. B. (1981a). The auditory bullae-swimbladder system in late stage herring larvae. *J. Mar. Biol. Ass. U.K.* 61:315-326.
- Blaxter, J. H. S., Denton, E. J. and Gray, J. A. B. (1981b). Acousticolateralis system in clupeid fishes. In: *Hearing and Sound Communication in Fishes*, ed. Tavolga, W. N., Popper, A.N., and Fay, R.R., pp. 39-59. New York: Springer Verlag.
- Bleckmann, H. (1993). The role of lateral line in fish behaviour. In: *Behaviour of teleost fishes*, ed Pitcher T. J., pp. 201-246. New York:Springer Verlag.
- Bleckmann, H. and Mogdans, J. (2014). Neuronal basis of source localisation and processing of bulk water flow with the fish lateral line. In: *Flow Sensing in Air and Water*, eds. Bleckman, H., Mogdans, J. and Coombs, S. L., pp. 371-398. New York: Springer Verlag.
- Bleckmann, H. and Zelick, R. (2009). Lateral line system of fish. *Integr. Zool.* 4:13-25.
- Bleckman, H., Breithaupt, T., Blickhan, R. and Tautz, J. (1991). The time course and frequency content of hydrodynamic events caused by moving fish, frogs, and crustaceans. *J. Comp. Physiol.* 168:749-757.
- Braun, C. B. and Grande, T. (2008). Evolution of Pheripheral Mechanisms for the Enhancement of Sound Reception. In: *Fish Bioacoustics*, eds. Webb, J. J., Fay, R. R. and Popper, A. N., pp. 99-144. New-York: Springer Verlag.
- Buwalda, R. J. A., Schuijf, A. and Hawkins, A. D. (1983). Discrimination by cod of sounds from opposing directions. *J. Comp. Physiol.* 150:175-184.

- Canfield, J. G. (2002). Functional evidence for visuospatial coding in the Mauthner neuron. *Brain Behav. Evol.* 67:188-202.
- Canfield, J. G. and Rose, J. G. (1996). Hierarchical sensory guidance of Mauthner-mediated escape responses in Goldfish (*Carassius auratus*) and chichlids (*Haplochromis burtoni*). *Brain Behav. Evol.* 48:137-156.
- Carter, C. G., McCarthy, I. D., Houlihan, D. F., Johnstone, R., Walsingham, M. V., and Mitchell, A. I. (1994). Food consumption, feeding behaviour, and growth of triploid and diploid Atlantic salmon, *Salmo salar L.*, parr. *Canadian Journal of Zoology* 72(4): 609-617.
- Casagrand, J. L., Guzik, A. L. and Eaton, R. C. (1999). Mauthner and reticulospinal responses to the onset of acoustic pressure and acceleration stimuli. *J. Neurophysiol.* 82:1422-1437.
- Denton, E. J. and Gray, J. A. B. (1980). Receptor activity in the utricle of the sprat. *J. Mar. Biol. Ass. U.K.* 60:717-740.
- Denton, E. J. and Gray, J. A. B. (1993). Stimulation of the acoustico-lateralis system of clupeid fish by external sources and their own movements. *Phil. Trans. R. Soc. Lond. B* 341: 113-127.
- De Vries, H. L. (1950). The mechanics of labyrinth otoliths. *Acta Oto-Lar.* 38:262-273.
- Domenici, P. (2006). The visuallay mediated escape response in fish: predicting prey responsiveness and the locomotor behaviour of predators and prey. *Mar. Fresh. Behav. Physiol.* 35:87-110.
- Eaton, R. C. and Emberley, D.S. (1991). How stimulus direction determines the trajectory of the Mauthner-initiated escape response in a teleost fish. *J. Exp. Biol.* 161:469-487.
- Eaton, R. C. and Popper, A. N. (1995). The octavolateralis system and Mauthner cell: interactions and questions. *Brain Behav. Evol.* 46:124-130.
- Eaton, R. C., Bombardieri, R. A. and Meyer, D. L. (1977). The Mauthner-initiated startle response in teleost fish. *J. Exp. Biol.* 66:65-81.
- Eaton, R. C., Canfield, J. C. and Guzik, A. L. (1995). Left-right discrimination of sound onset by the Mauthner system. *Brain Behav. Evol.* 46:165-179.
- Eaton, R. C., Lee, R. K. K. and Foreman, M. B. (2001). The Mauthner cell and other identified neurons of the brainstem escape network of fish. *Prog Neurobiol* 63:467-485.
- Faber, D. S. and Korn, H. (1975). Inputs from the posterior lateral line nerves upon the goldfish Mauthner cell. Evidence that the inhibitory components are mediated by interneurons of the recurrent collateral network. *Brain res.* 96:249-356.
- Faber, D. S., Fetcho, J. R. and Korn, H. (1989). Neural networks underlying the escape response in goldfish. *Ann. NY Acad. Sci.* 563:11-33.

- Faber D. S., Korn H. and Lin J. W. (1991). Role of medullary networks and postsynaptic membrane properties in regulating Mauthner cell responsiveness to sensory excitation. *Brain Behav. Evol.* 37:286-297.
- Fay, R. R. and Popper, A. N. (2012). Fish hearing: New perspectives from two 'senior' Bioacusticians. *Brain. Behav. Evol.* 79:2015-217.
- Fraser, T. W. K., Fjellidal, P. G., Skjæraasen, J. E., Hansen, T. and Mayer, I. (2012b). Triploidy alters brain morphology in pre-smolt Atlantic salmon *Salmo salar*: possible implications for behaviour. *Journal of Fish Biology* 81(7): 2199-2212.
- Gray, J. A. B. (1984). Interaction of sound pressure and particle acceleration in the excitation of the lateral-line neuromasts of sprat. *Proc. R. Soc. Lond. B* 220:299-325.
- Guzik, A. L., Eaton, R. C. and Mathis, D. W. (1999). A connectionist model of left-right sound discrimination by the Mauthner system. *J. Comput. Neurosci.* 6:121-144.
- Hanke, W. (2014). Natural hydrodynamic stimuli. In: *Flow Sensing in Air and Water*, eds. Bleckman, H., Mogdans, J. and Coombs, S. L., pp. 3-29. New York: Springer-Verlag.
- Kalmijn, A. J. (1988). Hydrodynamic and acoustic field detection. In: *Sensory Biology of Aquatic Animals*, eds. Atema, J., Fay, R. R., Popper, A. N. and Tavolga, W. N., pp. 83-130. New York: Springer-Verlag.
- Kalmijn, A. J. (1989). Functional evolution of lateral line and inner ear sensory systems. In: *The mechanosensory lateral line*, eds. Coombs, C., Görner, P. and Münz, H., pp. 187-216. Amsterdam: Elsevier.
- Karlsen, H. E. (1992a). The inner ear is responsible for detection of infrasound in the perch (*Perca fluviatilis*). *J. Exp. Biol.* 171:163-172.
- Karlsen, H. E. (1992b). Infrasound Sensitivity in the Plaice (*Pleuronectes platessa*). *J. Exp. Biol.* 171:173-187.
- Karlsen, H. E., Piddington, R. W., Enger, P. S. and Sand, O. (2004). Infrasound initiates directional fast-start escape in juvenile roach *Rutilus rutilus*. *J. Exp. Biol.* 207:4185-4193.
- Korn, H. and Faber, D. S. (1975). Inputs from the posterior lateral line nerves upon the goldfish Mauthner cell. Properties and synaptic localization of the excitatory component. *Brain Res.* 96:342-348.
- Korn, H. and Faber, D. S. (1996). Escape - brainstem and spinal cord circuitry and function. *Curr. Opin. Neurobiol.* 6:862-832.
- Ladich, F. (2010). Hearing: Vertebrates. In: *Encyclopedia of Animal Behaviour*, ed. Ladich, F., pp. 54-60. Vienna: Elsevier.



Ladich, F. (2014). Fish bioacoustics. *Curr. Opin. Neurobiol.*, 28:121-127.

Ladich, F. and Popper, A. N. (2004). Parallel evolution in fish hearing organs. In: *Evolution of the Vertebrate Auditory System*, eds. Manley, G. A., Popper, A. N. and Fay, R. R., pp. 95-127. New York: Springer.

Lewis, E. R. (1984). Inertial motion sensors. In: *Comparative Physiology of Sensory Systems*, eds. Bolis, L., Keynes, R. D. and Madrell, S. H. P., pp. 587-610. Cambridge: Cambridge University Press.

Medan, V. and Preuss, T. (2014). The Mauthner-cell circuit of fish as a model system for startle plasticity. *J. Physiol.* In press.

Mirjany, M. and Faber, D. S. (2011). Characteristics of the anterior lateral line nerve input to the Mauthner cell. *J. Exp. Biol.* 214:3368-3377.

Mirjany, M., Preuss, T. and Faber, D. S. (2011). Role of the lateral line mechanosensory system in directionality of goldfish auditory evoked response. *J. Exp. Biol.* 214:3358-3367.

Piddington, R. W. (1972). Auditory discrimination between compressions and rarefactions by goldfish. *J. Exp. Biol.* 56:403-419.

Popper, A. N. and Ketten, D. R. (2008). Underwater hearing. In: *The Senses: A Comprehensive Reference*, eds. Basbaum, A.I., Kaneko, A., Shepherd, G. M., Westheimer, G., Albright, T. D., Masland, T., Dallos, P. and Oertel, D., vol III, pp. 225-236. Vienna: Elsevier.

Popper, A. N. and Platt, C. (1979). The herring ear has a unique receptor pattern. *Nature* 228:832-833.

Popper, A. N., Fay, R. R., Platt, C. and Sand, O. (2003). Sound detection mechanisms and capabilities of teleost fishes. In: *Sensory Processing in Aquatic Environments*, eds. Collen, S. P. and Marshall, N.J., pp. 3-38. New York: Springer.

Rogers, P. H., Popper, A. N., Hastings, M. C. and Saidel, W. M. (1988). Processing of acoustics in the auditory system of bony fish. *J. Acoust. Soc. Am.* 83:338-349.

Sand, O. and Karlsen, H. E. (2000). Detection of infrasound and linear acceleration in fishes. *Philos. Trans. R. Soc. London* 355:1295-1298.

Schuijf, A. (1975). Directional hearing of cod under approximate free field conditions. *J. Comp. Physiol.* 98:307-332.

Schuijf, A. (1981). Models of acoustic localization. In: *Hearing and Sound Communication in Fishes*, eds. Tavalga, W. N., Popper, A. N., and Fay, R. R., pp. 267-310. New York: Springer Verlag.

Small, S. A. and Benfey, T. J. (1987). Cella size in triploid salmon. *J. Exp. Zool.* 241(3): 339-342.

Suresh, A. V. and Sheehan, R. J. (1998). Muscle fibre growth dynamics in diploid and triploid rainbow trout. *J. Fish Biol.* 52 (3): 570-587.

Swarup, H. (1959). Effect of triploidy on the body size, general organization and cellular structure in *Gasterosteus aculeatus (L)*. *J. Gen.* 56(2): 143-155.

Webb, J. F., Montgomery, J. C. and Mogdans J. (2007). Bioacoustics and the lateral line system of Fishes. In: *Fish Bioacoustics*, eds. Fay, R. R., Webb, J. F. and Popper, A. N., pp. 145-182. New York: Springer Verlag.

Zottoli, S. J. and Faber, D. S. (2000). The Mauthner cell: what has it taught us? *Neuroscientist* 6:26-38.